JIRRS
Journal International Review of Research Studies

Received: 02/05/2026 - **Accepted:** 26/08/2026
Vol: 01.09
DOI: 10.66104/bn5j2634
Pages: 1-49

Ca–Al Metallothermic Reduction: A Critical Review of Reductant Design, Reaction Pathways, Slag Engineering, and Scale-Up

Antonio Clareti Pereira, PhD
PhD in Chemical Engineering
University of São Paulo (USP)
Belo Horizonte, Minas Gerais, Brazil
E-mail: claretipereira@gmail.com
ORCID: https://orcid.org/0000-0001-8115-4279

Abstract

Calcium–aluminum (Ca–Al) alloys occupy a distinctive metallothermic design space between aluminothermy and calciothermy because Ca changes reductant activity, condensed–vapor partitioning, phase evolution, slag mineralogy, and metal–slag separation. This structured critical narrative review distinguishes direct pre-alloyed Ca–Al evidence from separately dosed Ca + Al, Ca-assisted aluminothermy, calciothermic/aluminothermic analogs, and $CaO–Al_2O_3$ slag studies. The review is evidence-classified but is not PRISMA-compliant; database-level retrieval counts, duplicate-removal counts, and exclusion logs were not retained, so corpus completeness cannot be independently reconstructed. It develops an author-developed Activities–Thermochemical response–Phase pathway–Slag and separation–Quality (A–T–P–S–Q) interpretive framework and two stoichiometric normalization descriptors: the reductant-equivalent ratio and the calcium share of oxygen-removal capacity. These descriptors normalize nominal oxygen-removal capacity but are not thermodynamic activity models or validated predictors of recovery. Recalculation of published compositions illustrates their value: a master alloy containing 69.4 wt.% Ca gives a calcium oxygen-removal share of about 0.504, whereas a Ca/Al mass ratio of 0.45 gives about 0.168. Across refractory and rare-metal systems, Ca–Al performance is governed by a coupled operating window rather than maximum Ca addition. Ca can strengthen reduction and reshape phase and slag pathways, but excessive Ca increases volatilization, containment, refractory, and safety burdens; maximum chemical conversion therefore need not coincide with maximum recovery or purity. Ca–Al should be selected only when its coupled benefits in redox strength, heat balance, product purity, or slag separation outweigh its volatility, containment, refractory, and safety burdens. Progress requires activity-informed thermodynamics, time-resolved phase analysis, closed Ca/Al/O balances, measured slag/interfacial properties, and prospective pilot validation.

Keywords: calcium–aluminum alloy; metallothermic reduction; calciothermy; aluminothermy; calcium aluminate slag; metal–slag separation

Highlights

CC BY

JIRRS
Journal International Review of Research Studies
Received: 02/05/2026 - **Accepted:** 26/08/2026
Vol: 01.09
DOI: 10.66104/bn5j2634
Pages: 1-49

- Ca–Al reductants should be compared by chemical activity and oxygen-removal equivalents, not only by alloy wt.% Ca.
- Intermediate Ca-bearing oxides and aluminides can either accelerate reduction or create diffusion-limiting product layers.
- The Ca/Al ratio simultaneously controls reduction potential, thermal response, Ca volatility, slag formation, and metal separation.
- Scale-up requires closure of Ca, Al, O, metal, slag, and off-gas balances while preserving the laboratory phase-separation regime.

1. Introduction

Metallothermic reduction remains strategically important wherever carbon contamination, carbide formation, low oxide stability, or highly refractory feedstocks constrain carbothermic processing. The classical thermodynamic foundation is the relative stability of oxides and the temperature dependence formalized through Ellingham-type analysis (Ellingham, 1944), while early calcium reduction of titanium illustrates the historical importance of calciothermy for highly stable oxides (Kroll, 1937). Aluminum is attractive because it is widely available, easy to dose, and capable of generating large reaction heats, whereas calcium offers even stronger oxygen affinity and can be removed from some products more readily due to its high vapor pressure and limited solubility in selected metals. These advantages, however, come with different process penalties. Aluminothermy can leave residual Al or generate highly refractory Al_2O_3-rich slags, while calciothermy increases sensitivity to moisture, volatilization, containment, and refractory interactions. Modern thermite literature further shows that heat release, phase formation, and transport are coupled rather than purely stoichiometric (Wang et al., 1993). Recent work on rare earths, Ti, Nb/Ta, V, W-containing feeds, and multicomponent alloys confirms that reductant selection is therefore not simply a ranking of standard free energies (Amon et al., 2024; Athelli & Reddy, 2026; Balakirev et al., 2021; Nababan et al., 2026; Okabe, 2020; Rafique, 2024).

Ca–Al alloys create a tunable intermediate regime. A pre-alloyed reductant changes the activities of both metals, the temperature at which a liquid reductant phase appears, and the distribution of Ca between condensed and vapor phases. It also shifts oxidation products from a single-oxide system to $CaO–Al_2O_3$-based slags, where calcium aluminates can strongly modify the liquidus temperature, viscosity, density, and wetting. Direct Ca–Al evidence remains limited, but reduction of Sc_2O_3 with Al–Ca alloys and recent wolframite and coltan studies using Ca–Al master alloys establish alloy-specific thermochemical and phase-pathway effects (Lee et al., 2024; Pikulin, Galkova, et al., 2026; Pikulin, Tyushnyakov, et al., 2026). Historical pilot- and full-scale calcium–

CC BY

JIRRS
Journal International Review of Research Studies
Received: 02/05/2026 - **Accepted:** 26/08/2026
Vol: 01.09
DOI: 10.66104/bn5j2634
Pages: 1-49

aluminothermal niobium production provides complementary scale-relevant evidence for separately dosed Ca + Al (Gorkunov & Munter, 2007). Ca-assisted aluminothermic Ti chemistry, conventional aluminothermy, and Si–Ca–Al alloy refining are used as adjacent evidence rather than as substitutes for direct alloy data (Balakirev et al., 2021; Cai et al., 2026; Emil-Kaya et al., 2024).

The scientific difficulty is that the nominal Ca/Al ratio is not the state variable that directly controls the reaction. Calcium and aluminum activities can deviate substantially from ideal-solution behavior, and Ca may leave the condensed reaction zone by vaporization. At the same time, the feed can transform through partially reduced oxides, Ca-containing ternary oxides, aluminides, or other intermetallics before a recoverable metal phase develops. Studies of tantalate, coltan, wolframite, cassiterite, niobium oxides, and complex refractory systems repeatedly show that phase history matters as much as final equilibrium (Gulyaeva, Sergeeva, et al., 2022; Gulyaeva, Udoeva, et al., 2022; Kryzhanov & Orlov, 2023; Pikulin, Galkova, et al., 2026; Pikulin, Tyushnyakov, et al., 2026; Tyushnyakov et al., 2021).

The engineering consequence is equally important: chemical reduction and physical metal recovery are separate performance dimensions. A highly reduced system can still lose metal as small droplets, intermetallic fragments, or metal trapped in a partially solid slag. Conversely, a moderately reducing composition may yield a lower-viscosity slag and better coalescence, resulting in a higher recoverable yield. Contemporary work on thermite product separation, CuW metallothermy, silicon production, and liquid-metal droplet behavior supports treating separation as part of the reaction design rather than as a downstream afterthought (Bullón et al., 2025; Cheng et al., 2024; Pereira, 2026; Song et al., 2021).

Accordingly, this review asks: how do Ca activity, Al activity, Ca/Al ratio, temperature, pressure, intermediate-phase formation, and slag chemistry jointly determine conversion, metal recovery, and product purity in Ca–Al metallothermic reduction? The review adopts a process-metallurgy decision-science logic rather than a meta-analytic logic: evidence is weighted by mechanistic proximity and used to define decision variables, inference boundaries, and validation requirements. It does not assume that Ca–Al is universally superior to Al or Ca. Instead, it identifies where the mixed system creates genuine process leverage, where it adds complexity without benefit, and which measurements are required to decide between the three reductant strategies.

Figure 1 distinguishes the evidence classes used throughout this review. This classification is necessary because a pre-alloyed Ca–Al reductant is not

CC BY

JIRRS
Journal International Review of Research Studies
Received: 02/05/2026 - **Accepted:** 26/08/2026
Vol: 01.09
DOI: 10.66104/bn5j2634
Pages: 1-49

thermodynamically or kinetically identical to adding Ca and Al separately, and neither is equivalent to adding CaO or $CaCl_2$ to an aluminothermic charge.

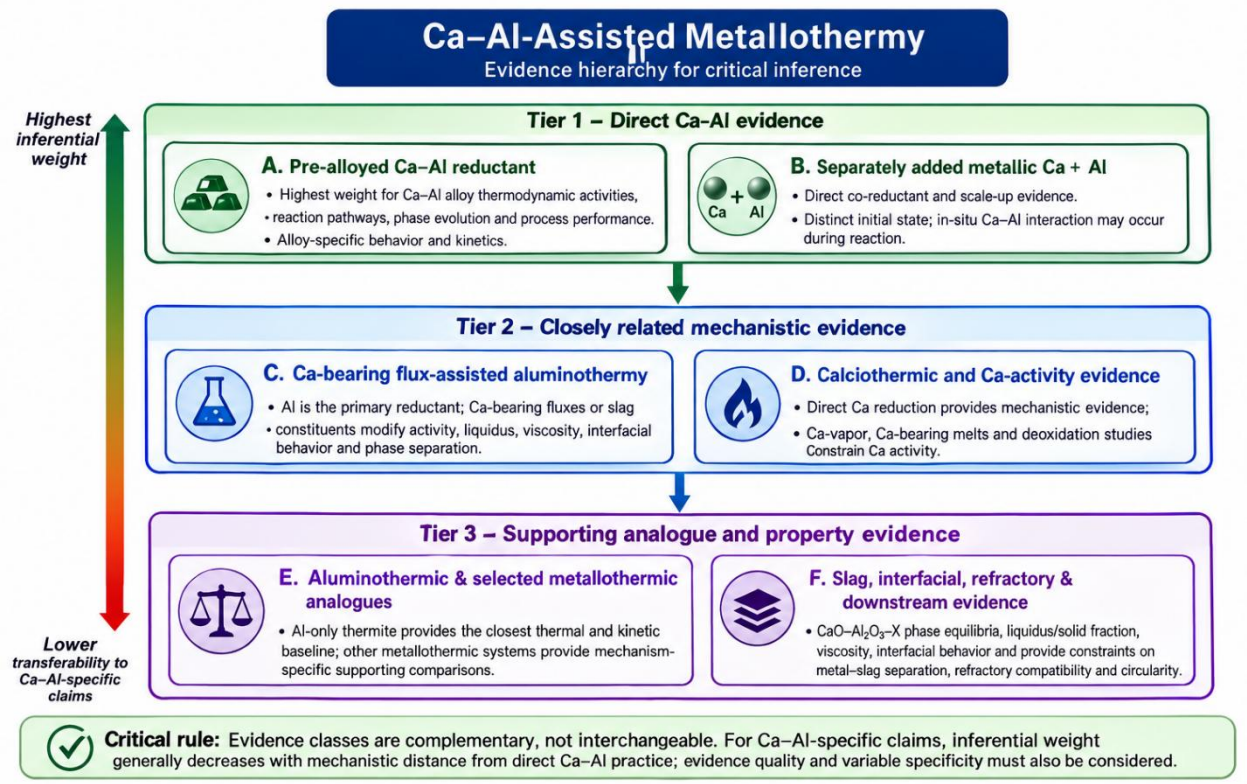


Figure 1. *Classification of Ca–Al-assisted metallothermic processes*
Note. Author's synthesis based on Gorkunov and Munter (2007), Lee et al. (2024), Cai et al. (2026), Makrovets et al. (2022), Pikulin, Galkova, et al. (2026), Pikulin, Tyushnyakov, et al. (2026), and the slag/interfacial literature summarized in Table 1. No graphic element was directly reproduced.

Figure 1 therefore establishes a six-class hierarchy of inference that is identical to Table 1. Classes A and B carry the greatest weight for Ca–Al-specific performance claims, Class C isolates Ca-assisted aluminothermy, and Classes D–F provide bounded thermodynamic, metallothermic, slag/interfacial, and downstream evidence. This structure reduces the risk of transferring a mechanism observed in a simpler analog directly to a multicomponent Ca–Al process.

2. Review Methodology and Evidence Classification

2.1 Scope and search logic

CC BY

JIRRS
Journal International Review of Research Studies

Received: 02/05/2026 - **Accepted:** 26/08/2026
Vol: 01.09
DOI: 10.66104/bn5j2634
Pages: 1-49

This review was structured as a critical narrative synthesis with a core literature window of January 2020–August 2026. The search was not restricted to a single bibliographic database; instead, structured keyword searches were conducted through publisher search interfaces and CrossRef-indexed metadata, followed by backward and forward citation chaining. Searches and metadata checks were finalized in August 2026. Five operational search blocks were used: (1) ("Ca–Al" OR "Al–Ca" OR "calcium aluminum") AND ("metallothermic reduction" OR aluminothermal OR aluminothermy); (2) (calciothermic OR "calcium vapor") AND (refractory OR "rare metal" OR niobium OR tantalum OR tungsten OR titanium OR vanadium); (3) (aluminothermic OR thermite) AND (CaO OR $CaCl_2$ OR slag OR separation OR "calcium assisted"); (4) ("CaO–Al_2O_3" OR "calcium aluminate") AND ("phase equilibrium" OR liquidus OR viscosity OR wetting OR dissolution); and (5) ("calcium aluminothermal" OR "calcium-aluminothermic") AND (pilot OR industrial OR niobium OR tantalum OR tungsten).

Inclusion required either direct pre-alloyed Ca–Al evidence, separately dosed Ca + Al evidence, or mechanistically transferable information on activity, phase evolution, Ca vapor transport, calcium-aluminate slags, metal–slag separation, product purity, reactor behavior, downstream slag treatment, or scale-up. Duplicate reports, studies without usable process or phase information, and calcium-containing systems lacking a defensible mechanistic link were excluded from performance claims. The contemporary evidence corpus contains 93 scholarly publications; Gorkunov and Munter (2007) was retained as a documented pre-2020 exception because it reports pilot- and full-scale calcium–aluminothermal niobium production, bringing the evidence-class corpus to 94 scholarly publications. NFPA 484 (2022) is cited separately as a safety standard and is not counted in the scholarly corpus. Five additional pre-2020 sources added during revision—Ellingham (1944), Kroll (1937), Turkdogan (1983), Verein Deutscher Eisenhüttenleute (1995), and Wang et al. (1993)—serve only as foundational contextual anchors and are not included in the 94-source evidence-class corpus. This is not a PRISMA-compliant systematic review: database-level retrieval counts, duplicate-removal counts, and a source-by-source exclusion log were not retained during the original search, so corpus completeness and a PRISMA flow cannot be independently reconstructed. Auditability of the included evidence is instead provided by explicit search blocks, inclusion logic, evidence weighting, and the complete source-by-source evidence map in Supplementary Table S1.

Mechanistic analogs are intentionally included but explicitly bounded. Aluminothermic and other metallothermic studies inform heat generation, reaction pathways, separation, and

CC BY

JIRRS
Journal International Review of Research Studies
Received: 02/05/2026 - **Accepted:** 26/08/2026
Vol: 01.09
DOI: 10.66104/bn5j2634
Pages: 1-49

scale-up (Balakirev et al., 2021; Fu et al., 2024; Kudyba et al., 2021; Philipson et al., 2024a, 2024b; Zhu et al., 2024); calciothermic, Ca-vapor, and Ca-containing thermodynamic/deoxidation studies constrain Ca activity, transport, impurity behavior, and phase stability (Kasimtsev et al., 2020; Kim & Lim, 2022; Makrovets et al., 2022; Orlov & Kryzhanov, 2020, 2021, 2024; Wang et al., 2020; Yao et al., 2023); and calcium-aluminate/interfacial studies constrain slag interpretation and downstream recovery (Azof et al., 2020; Huo et al., 2026; Liu et al., 2024a, 2024b; Qiu et al., 2023; Zhi et al., 2022). These sources are used to bound mechanisms and engineering variables, not as evidence of identical Ca–Al alloy performance.

2.2 Evidence classes and critical weighting

Table 1 summarizes the six evidence classes applied to the 94-publication scholarly corpus. The distinction is methodological rather than semantic: the same variable can have different meaning depending on whether Ca is present as a pre-alloyed metallic component, a separately dosed reductant, a flux or slag modifier, a vapor-phase reagent, or only within a mechanistic analogue. Direct alloy and separately dosed Ca + Al evidence receives the greatest weight for Ca–Al-specific performance claims; thermodynamic, metallothermic, slag/interfacial, and downstream studies are used primarily to constrain mechanism, transport, separation, circularity, and scale-up logic. Evidence classification and critical weighting were performed by the sole author. No independent second coder was involved; consequently, no Cohen's kappa, Krippendorff's alpha, or other inter-rater statistic is reported. The A–F map must therefore be interpreted as single-reviewer interpretive coding rather than as an independently validated coding instrument. Supplementary Table S1 makes each source-level assignment, process role, and transferability limitation explicit, allowing readers to audit or reclassify individual entries.

Table 1. *Evidence hierarchy used in the critical review*

Evidence class	Defining feature	Primary use in this review	Representative sources
A. Direct Ca–Al reductant	Pre-alloyed Al–Ca used as metallic reductant	Highest-weight evidence for alloy activity, product chemistry, Ca/Al interaction, and direct phase pathways	Lee et al. (2024). Pikulin, Galkova, et al. (2026); Pikulin, Tyushnyakov, et al. (2026)

CC BY

JIRRS
Journal International Review of Research Studies

Received: 02/05/2026 - **Accepted:** 26/08/2026
Vol: 01.09
DOI: 10.66104/bn5j2634
Pages: 1-49

Evidence class	Defining feature	Primary use in this review	Representative sources
B. Separate Ca + Al reductants	Metallic Ca and Al supplied separately	Direct evidence for Ca/Al cooperation, dosage, and scale-relevant response, but not identical to a pre-alloyed reductant	Gorkunov & Munter (2007)
C. Ca-assisted aluminothermy	Al is primary reductant; $CaO/CaCl_2$ or Ca-bearing slag modifies the route	Strong evidence for phase/slag effects; weak evidence for metallic Ca activity	Cai et al. (2026); Cheng et al. (2023, 2024)
D. Calciothermic / Ca-containing thermodynamic analogues	Metallic Ca, Ca vapor, Ca hydride, Mg–Ca melt, or Ca-containing deoxidation/thermodynamic systems	Constrains Ca activity, volatility, transport, impurity behavior, and equilibrium response	Athelli & Reddy (2026); Kim & Lim (2022); Makrovets et al. (2022); Kryzhanov & Orlov (2023)
E. Aluminothermic / other metallothermic analogues	Al-only thermite or other metallothermic reduction without direct Ca–Al alloy evidence	Heat generation, kinetic/phase baselines, metal formation, and scale-up analogs	Amon et al. (2024); Balakirev et al. (2021); Fu et al. (2024); Nababan et al. (2026)
F. Slag, interfacial, and downstream evidence	$CaO–Al_2O_3–MO_x$ phase equilibria, viscosity, wetting, dissolution, slag treatment, or valorization	Constrains metal–slag separation, refractory interaction, slag design, recovery, and circularity	Ma et al. (2025). C. Wang et al. (2025); X. Zhang et al. (2022); Huang et al. (2025)

Note. Author's evidence classification based on the cited literature. Direct pre-alloyed Ca–Al evidence is weighted most heavily for alloy-specific claims; separately dosed Ca + Al is retained as a distinct class; classes D–F constrain thermodynamics, mechanisms, slag/interfacial behavior, downstream treatment, and engineering interpretation rather than implying identical industrial behavior.

Table 1 prevents a common error in emerging-process reviews: extrapolating a mechanism observed in a simpler analog directly to a multicomponent industrial charge.

CC BY

JIRRS
Journal International Review of Research Studies

Received: 02/05/2026 - **Accepted:** 26/08/2026
Vol: 01.09
DOI: 10.66104/bn5j2634
Pages: 1-49

For example, calcium vapor deoxidation establishes that gas-phase Ca can be reactive, but it does not by itself quantify Ca evaporation from a self-heating Ca–Al metallothermic bed. Likewise, $CaO–Al_2O_3$ phase diagrams are necessary for slag design but cannot predict the dynamic local composition created during a fast thermite reaction.

Table 1A. Direct Ca–Al evidence versus analog evidence for major claims

Major claim	Highest supporting evidence	Evidence status	Inference boundary
Pre-alloyed Ca–Al changes thermochemical and phase pathways	Lee et al. (2024); Pikulin, Galkova, et al. (2026); Pikulin, Tyushnyakov, et al. (2026)	Direct Class A	Observed in three system-specific studies; no universal optimum or recovery law is established.
Separately dosed Ca + Al can operate at scale	Gorkunov & Munter (2007)	Direct Class B, scale-relevant	Industrial Nb evidence; separate dosing is not thermodynamically identical to a pre-alloyed Ca–Al master alloy.
Ca-bearing intermediates can accelerate or impede reduction	Pikulin studies; Cai et al. (2026); tantalate/niobate analogues	Mixed: A plus C–D	Direct in selected Class A feeds; broader generalization is a bounded mechanistic hypothesis.
Calcium-aluminate slag can modify separation	Class F phase/property studies; Cheng et al. (2023, 2024)	Analog/assisted C–F	Phase/property direction is transferable; quantitative viscosity, wetting, and settling thresholds are system-specific.
A–T–P–S–Q and scale-up sequence organize engineering decisions	Author synthesis constrained by Classes A–F	Interpretive framework	Proposed reporting/decision scaffold, not a validated predictive or industrial model.
Ca–Al can improve environmental/economic performance	No direct comparative TEA/LCA evidence	Not established	Any advantage remains conditional on recovery, energy, Ca loss, containment, refining, slag credits, and functional unit.

Note. Class A denotes direct pre-alloyed Ca–Al evidence; Class B denotes separately dosed metallic Ca + Al; Classes C–F are bounded assisted, thermodynamic, metallothermic, slag/interfacial, or downstream analogs. The table reports evidentiary status rather than statistical certainty.

2.3 Criteria for critical synthesis

Evidence was interpreted against five questions: (1) what is the effective reducing potential of the metallic phase; (2) how is reaction heat generated, retained, or lost; (3) what intermediate phases control the path to metal; (4) what slag state permits metal coalescence and separation; and (5) what product quality and recovery are obtained after accounting for Ca/Al partitioning. Each study was assigned one primary evidence class according to its dominant process role; where a source informed more than one

CC BY

JIRRS
Journal International Review of Research Studies
Received: 02/05/2026 - **Accepted:** 26/08/2026
Vol: 01.09
DOI: 10.66104/bn5j2634
Pages: 1-49

mechanism, secondary uses are noted in Supplementary Table S1 rather than used to elevate its evidentiary weight. Studies emphasizing precursor effects, in situ mechanisms, thermodynamic simulation, or phase transformations were given particular weight in mechanistic sections (Coetsee et al., 2026; Deng et al., 2026; Disconzi et al., 2025; Sergeeva et al., 2022). This conservative assignment rule is intended to make the inference boundary visible, not to imply statistical objectivity of the coding.

3. Fundamentals of the Ca–Al Reductant System

3.1 Stoichiometric oxygen-removal basis

For a generic oxide M_xO_Y, the limiting idealized reactions can be written as follows. These expressions are accounting identities for oxygen transfer; they do not imply that the real mechanism is a single-step reaction.

$$M_xO_Y + y\,Ca \rightarrow x\,M + y\,CaO$$

$$M_xO_Y + (2y/3)\,Al \rightarrow x\,M + (y/3)\,Al_2O_3$$

For a mixed Ca–Al reductant, the ideal oxygen balance is $\alpha + 1.5\beta = y$, where α and β are the moles of Ca and Al assigned to oxygen removal per mole of M_xO_Y. This representation is more useful than reporting only mass percent alloy addition because it compares compositions on a common reducing-capacity basis. It also exposes excess-reductant conditions that can increase residual alloying elements, vaporization, or refractory attack.

3.2 Activities rather than nominal composition

The thermodynamic force of Ca–Al reduction depends on chemical activities rather than elemental fractions. Strong interactions within metallic melts and intermetallic formation mean that aCa and aAl can depart from ideal mole-fraction behavior. This issue is familiar in calcium treatment of Al-deoxidized steels, where Ca–Al–O equilibria and total Ca/O control are used to interpret inclusion transformations (Geng et al., 2020; Wang et al., 2026). The same principle is even more important in metallothermy because the reductant may pass simultaneously through solid intermetallics, a liquid alloy, and a Ca-rich vapor.

Makrovets et al. (2022) showed, from a deoxidation-thermodynamics perspective, that alkaline-earth-metal reducing ability should be evaluated in the presence of aluminum rather than as isolated pure elements; this study is therefore treated here as a Class D thermodynamic analog rather than as direct mixed-reductant evidence. Calcium-alloy treatment of steel similarly demonstrates that Ca can redistribute impurity chemistry in Al-containing metallic systems (Yao et al., 2023). Direct reduction of Sc_2O_3 using Al–Ca alloys equilibrated with a Ca-bearing flux further demonstrates that the effective chemical state of Ca can be controlled by coupled alloy/slag equilibria (Lee et al., 2024). Thus, a

CC BY

JIRRS
Journal International Review of Research Studies
Received: 02/05/2026 - **Accepted:** 26/08/2026
Vol: 01.09
DOI: 10.66104/bn5j2634
Pages: 1-49

report stating only “Ca–Al alloy containing 70 wt.% Ca” is incomplete unless alloy phase state, temperature, atmosphere, dosage relative to oxygen demand, and pressure are also given.

3.2.1 Practical estimation and validation of Ca and Al activities

Future Ca–Al studies should estimate activities through a staged workflow rather than assume ideal mixing. First, the metallic phase constitution should be established at the reaction temperature, including solid intermetallic, liquid-alloy, and possible two-phase regions. Second, CALPHAD or another assessed thermodynamic description should be used, where available, to estimate aCa and aAl and their sensitivity to composition and temperature. Third, because Ca may partition strongly to the vapor phase, the calculated condensed-phase state should be checked against Ca vapor pressure and the actual reactor pressure. Fourth, alloy–slag equilibrium experiments, vapor-pressure measurements, or activity-coefficient measurements should be used to validate calculations in composition regions central to process design. Finally, sensitivity analysis should propagate uncertainty in activities into predicted oxygen potential and phase stability. Existing databases are useful for selected Ca–Al–O and $CaO–Al_2O_3–MO_x$ subsystems, but they are not universally validated for rapidly reacting, multicomponent metallothermic beds; database extrapolation should therefore be identified explicitly and tested experimentally where it controls a process conclusion.

3.3 Normalized descriptors for comparing studies

Two descriptors are proposed for cross-study comparison. The first is the reductant-equivalent ratio, R_eq, defined as the supplied oxygen-removal equivalents divided by the stoichiometric oxygen atoms associated with the reducible feed. The second is the calcium share of reducing capacity, χ_Ca, which expresses how much of the nominal oxygen-removal capacity is assigned to Ca.

$R_{eq} = (n_{Ca} + 1.5\, n_{Al}) / n_{O,stoich}$

$\chi_{Ca} = n_{Ca} / (n_{Ca} + 1.5\, n_{Al})$

χCa = 0 indicates pure aluminothermy, χCa = 1 indicates pure calciothermy. Intermediate values show Ca's reducing capacity, not its mass fraction, useful for comparing Al-rich alloys, Ca-rich alloys, and reductants on the same oxygen basis. For instance, recalculating a Ca–Al alloy with 69.4 wt.% Ca shows χCa = 0.504, not 0.694. Similarly, a Ca/Al ratio of 0.45 equals χCa = 0.168. These examples prove that mass composition and oxygen-removal capacity are not interchangeable.

Box 1. Descriptor status and limits

CC BY

JIRRS
Journal International Review of Research Studies

Received: 02/05/2026 - **Accepted:** 26/08/2026
Vol: 01.09
DOI: 10.66104/bn5j2634
Pages: 1-49

Descriptor status R_eq and χCa are stoichiometric normalization tools for nominal oxygen-removal capacity. They are not thermodynamic activity models, kinetic models, or validated predictors of conversion, recovery, yield, or purity. Nominal oxygen-removal capacity can differ from effective reducing capacity when Ca volatilizes, reductant is captured by slag or refractory reactions, residual reductant remains unreacted, intermediate phases sequester oxygen or metal, or reaction is incomplete. Therefore, R_eq and χCa should be reported together with temperature, pressure, phase state, mass loss, Ca/Al partitioning, and closed material balances.

Table 2 applies the normalized descriptors to direct or scale-relevant evidence where the reported composition permits calculation. Unrecoverable values are left explicit rather than inferred from incomplete charge descriptions.

Table 2. *Quantitative anchors for direct and scale-relevant Ca–Al metallothermic evidence*

Source / class	System & normalization	Conditions	Key process outcome	Evidence limit
Gorkunov & Munter (2007) B	Nb_2O_5; Ca + Al; Ca/Al=0.45 χCa=0.168	Pilot/full scale; →Ar	>90% Nb; 4.4% Al; $3CaO·5Al_2O_3$ slag; ~2000 kg ingots	R_eq not uniquely reconstructible
Lee et al. (2024) A	Sc_2O_3; Al–Ca/CaO–$CaCl_2$	1273–1623 K	Max. 3.98 wt.% Sc; Ca–CaO potential controls recovery	No single transferable χCa/R_eq
Pikulin, Galkova, et al. (2026) A	Wolframite; Ca–Al master alloy	Thermochemical + phase analysis	Thermal effect +4.3%; T_ad +~390 °C; Ca tungstate/aluminides	R_eq unavailable
Pikulin, Tyushnyakov, et al. (2026) A	Coltan; 69.4 wt.% Ca → χCa=0.504	800–1450 °C	Ca intermediates can form barriers; parent phase absent at 1450 °C	R_eq unavailable

Note. χCa values were recalculated from reported Ca and Al masses using the definition in Section 3.3. R_eq is reported only when the stoichiometric oxygen demand and total supplied reducing equivalents can be reconstructed without assumption. “Not reconstructible” is therefore a reporting limitation, not a zero value.

The comparison shows why normalization matters: 69.4 wt.% Ca corresponds to χCa ≈ 0.504, not 0.694. It also exposes a reporting gap—without a complete charge oxygen balance, R_eq cannot be reconstructed for several direct studies, so nominal alloy composition alone cannot establish under- or over-stoichiometry.

Figure 2 places these descriptors inside the author-developed A–T–P–S–Q interpretive framework. The framework is a reporting and decision scaffold intended to prevent process optimization from stopping at equilibrium conversion and to force explicit

CC BY

JIRRS
Journal International Review of Research Studies
Received: 02/05/2026 - **Accepted:** 26/08/2026
Vol: 01.09
DOI: 10.66104/bn5j2634
Pages: 1-49

consideration of heat, phases, separation, and quality. It has not been prospectively validated as a quantitative predictor of recovery or as an industrial design model.

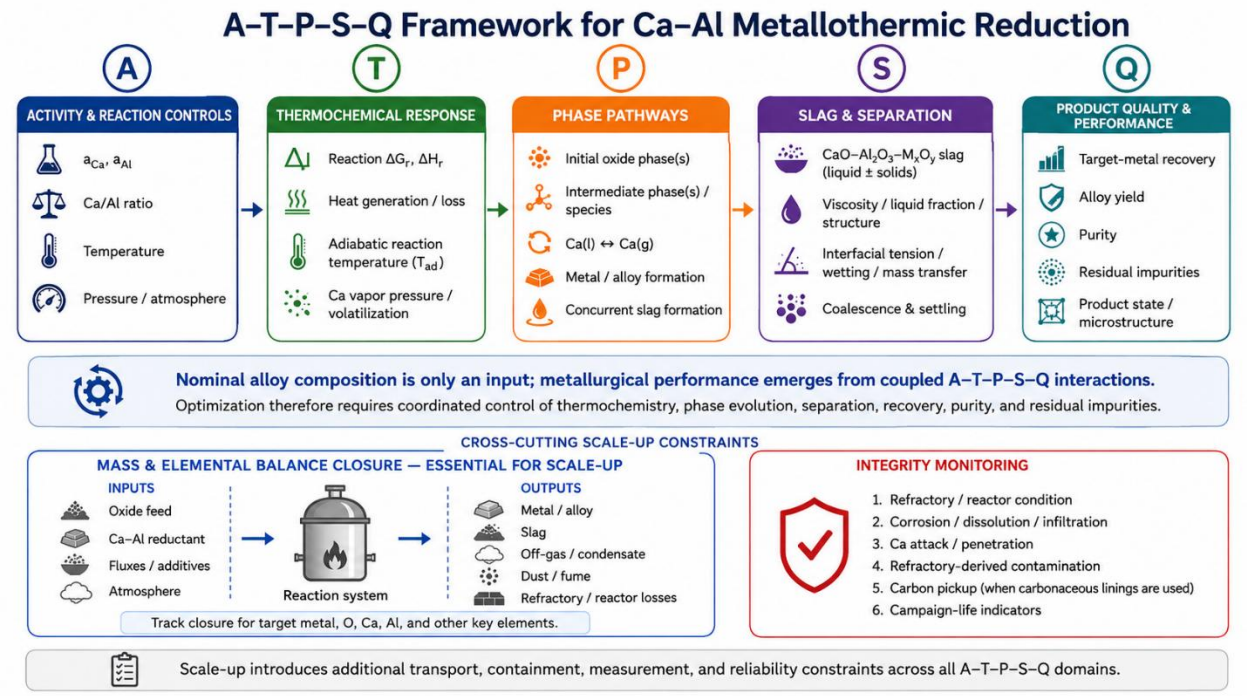


Figure 2. *A–T–P–S–Q framework for Ca–Al metallothermic reduction*
Note. Author's synthesis based on Makrovets et al. (2022), Deng et al. (2026), Pikulin, Galkova, et al. (2026) and Pikulin, Tyushnyakov, et al. (2026), Pereira (2026), and Wang et al. (2026). No graphic element was directly reproduced.

Figure 2 also clarifies why Ca–Al metallurgy is inherently coupled. A change in composition alters activities (A), which in turn changes the thermochemical response (T), which in turn changes the sequence and persistence of phases (P). Those phases define the slag state and physical separation behavior (S), ultimately controlling recovery, yield, product state, purity, and residual impurities (Q). Accordingly, the relationships shown in Figure 2 indicate that hypothesized causal links should be tested experimentally rather than fitted with universal response functions.

4. Feedstocks, Target Metals, and Product Classes

4.1 Simple oxides and rare-earth systems

Simple oxides provide the clearest thermodynamic benchmark because oxygen transfer can be interpreted without first resolving a complex mineral lattice. Recent examples include aluminothermic CeO_2 reduction, calciothermic Sm_2O_3 and Nd extraction, calcium-

CC BY

JIRRS
Journal International Review of Research Studies
Received: 02/05/2026 - **Accepted:** 26/08/2026
Vol: 01.09
DOI: 10.66104/bn5j2634
Pages: 1-49

vapor reduction of V_2O_3, and Ca–Al reduction of Sc_2O_3 (Amon et al., 2024; Athelli & Reddy, 2026; Sahoo et al., 2024; Wang et al., 2020; Lee et al., 2024). Rare-earth systems also demonstrate a central tradeoff: highly stable oxides demand strong reductants, yet the product can be reoxidized or contaminated by the oxide/halide medium if phase separation is poor. Karati et al. (2025) broaden this discussion by showing the continuing search for rare-earth routes that avoid aggressive fluoride chemistry.

4.2 Complex refractory minerals and mixed oxides

Complex oxides are especially relevant to Ca–Al because the reductant can destabilize the parent mineral by forming new Ca-bearing phases before the target metal is fully reduced. Tantalite, iron/manganese tantalates, coltan, wolframite, cassiterite, and niobium oxide compounds provide representative examples in the literature considered here (de Oliveira et al., 2023; Gulyaeva, Sergeeva, et al., 2022; Gulyaeva, Udoeva, et al., 2022; Kryzhanov & Orlov, 2023; Pikulin, Galkova, et al., 2026; Pikulin, Tyushnyakov, et al., 2026; Tyushnyakov et al., 2021). In such feeds, “conversion of the original mineral” is not equivalent to “formation of recoverable metal,” because disappearance of the feed phase can simply indicate transformation into a more or less reducible intermediate. Recent reviews of niobium pyrometallurgy likewise emphasize that reduction and purification must be assessed together when high-purity Nb is the target (Jiang et al., 2026). Tungsten-residue recovery studies also show that thermodynamic reducibility must be assessed together with impurity partitioning and residue treatment when W-bearing secondary feeds are considered (Su et al., 2021).

The recent coltan work is particularly instructive. Pikulin, Tyushnyakov, et al. (2026) reported that a Ca–Al master alloy containing 69.4 wt.% Ca changed the reduction sequence relative to Al, promoted Ca-bearing intermediate phases, and generated diffusion-limiting phases at intermediate temperatures; $CaAl_2$ was identified as a plausible later reducing participant within the evolving metallic/intermetallic assemblage. The wolframite study likewise showed a mechanism that differs from simple aluminothermy, involving calcium tungstate-type phases and aluminides prior to subsequent reduction (Pikulin, Galkova, et al., 2026). These observations justify treating phase evolution as an independent design variable rather than embedding it within a single global kinetic model.

4.3 Alloy and intermetallic production

Metallothermy can target an alloy directly rather than an elemental metal. Examples include Ti–Al-based products, TiFe, Cr_2Ta, $LaNi_5$, Mo–Ti–Ta–Cr powders, WCu composites, V–Ni alloys, and complex W–Mo–Cr alloys (Cheng, K.-X. Song, Z.-W. Song,

CC BY

JIRRS
Journal International Review of Research Studies
Received: 02/05/2026 - **Accepted:** 26/08/2026
Vol: 01.09
DOI: 10.66104/bn5j2634
Pages: 1-49

et al., 2022; Cheng, Z.-W. Song, K.-X. Song, et al., 2022; Cheng, Z.-W. Song, Wang, et al., 2022; Guryanov et al., 2023; Makhambetov et al., 2026; Rasheed et al., 2026; Teslia et al., 2026; Yudin et al., 2024, 2025; Zeng et al., 2026). In these cases, the desired product composition modifies the reductant problem: residual Al may be acceptable or beneficial for an aluminide but unacceptable for high-purity Nb or Ta, while Ca may be advantageous if it can be removed during cooling or vacuum treatment.

Across the feed and product classes considered here, Ca–Al is most likely to create value where more than oxygen affinity is required. Complex minerals, products sensitive to residual Al, and systems in which reductant oxides can be converted into a fluid calcium-aluminate slag are stronger candidates than simple oxides already reduced efficiently by conventional aluminothermy.

5. Thermodynamics and Thermochemical Response

5.1 Oxygen affinity, Gibbs energy, and activity effects

The conventional thermodynamic starting point is the relative stability of CaO, Al_2O_3, and the target oxide. Ellingham-type analysis provides the foundational oxygen-potential comparison, but the useful criterion is the reaction Gibbs energy at the actual activities of reactants and products rather than a pure-component ranking (Ellingham, 1944). Calcium generally occupies a stronger reducing position than aluminum for many refractory oxides, while early calciothermic titanium practice illustrates both the power and the handling burden of Ca (Kroll, 1937). In a Ca–Al alloy, lowering aCa through alloying can moderate Ca activity while still providing a stronger reducing contribution than Al alone. This tunability is a potential advantage, but it means that pure-component Ellingham comparisons are insufficient (Makrovets et al., 2022; Rafique, 2024; Zhi et al., 2022). The broader OS-process literature provides an additional calciothermic benchmark for the thermodynamic and transport roles of calcium in oxide reduction (Suzuki & Ono, 2025), while classical thermite analysis emphasizes that adiabatic heat release and phase formation must be treated together (Wang et al., 1993).

Thermodynamic assessments and phase-equilibrium studies in CaO–Al_2O_3–Sc_2O_3, CaO–Al_2O_3–VO_x, and CaO–Al_2O_3–La_2O_3 systems show that the oxide products participate in non-ideal, multicomponent phases rather than remaining as separate CaO and Al_2O_3 end-members (Huo et al., 2026; Liu et al., 2024a, 2024b; Qiu et al., 2023; Xie et al., 2025, 2026; Zhi et al., 2022). The reaction quotient must therefore account for phase stability on the slag side as well as metallic activities on the reductant side.

5.2 Pressure and calcium volatility

CC BY

JIRRS
Journal International Review of Research Studies
Received: 02/05/2026 - **Accepted:** 26/08/2026
Vol: 01.09
DOI: 10.66104/bn5j2634
Pages: 1-49

Pressure is a first-order variable because calcium can participate as a condensed metal, a dissolved alloy component, or a vapor. Calcium-vapor reduction of niobium and vanadium oxides and surface deoxidation of Ti alloys show that gaseous Ca can transfer oxygen effectively (Kim & Lim, 2022; Kryzhanov & Orlov, 2023; Wang et al., 2020). In a self-heating Ca–Al charge, however, vaporization can either extend reaction into porous regions or remove reductant from the intended reaction zone. Vacuum may enhance Ca transport and post-reaction removal, but it can also increase reductant loss unless vapor is recirculated or the reactor geometry favors contact with the oxide.

5.3 Heat generation, heat sinks, and adiabatic temperature

Aluminothermic reactions are valued partly because they can become self-sustaining. The actual temperature, however, depends on sensible heat, latent heat, heat absorbed by inert additions, slag melting, vaporization, vessel losses, and the heat capacities of both products and unreacted feed. Industrial magnesium retort studies demonstrate the sensitivity of aluminothermic efficiency to charge and heat-transfer conditions; manganese-slag aluminothermy provides an additional benchmark for charge chemistry and reduction behavior; and the use of Al_2O_3 as a deliberate heat sink in vanadium thermite processing illustrates that lowering peak temperature can be beneficial when thermal runaway or volatile losses threaten process control (Fu et al., 2024; Kudyba et al., 2021; Jain & Awasthi, 2025).

Quantitative anchors illustrate system specificity. Pikulin, Galkova, et al. (2026) reported that a Ca–Al master alloy increased the calculated thermal effect of wolframite reduction by 4.3% and the adiabatic temperature by about 390 °C relative to their aluminothermic case. Gorkunov and Munter (2007) identified a favorable Ca/Al mass ratio of 0.45 during Nb_2O_5 reduction, yielding>90% Nb, 4.4% Al, and a $3CaO{\cdot}5Al_2O_3$-rich slag. Lee et al. (2024) studied Al–Ca/Sc_2O_3 equilibria at 1273–1623 K and obtained up to 3.98 wt.% Sc, with recovery governed by the Ca–CaO oxygen potential. These results are system-specific but demonstrate that Ca/Al changes redox strength, heat, alloy/flux equilibrium, and slag state simultaneously.

Figure 3 summarizes the expected qualitative competition as Ca share increases. The curves are intentionally non-quantitative because the location of the optimum depends on oxide stability, alloy thermodynamics, pressure, and slag composition.

CC BY

JIRRS
Journal International Review of Research Studies
Received: 02/05/2026 - **Accepted:** 26/08/2026
Vol: 01.09
DOI: 10.66104/bn5j2634
Pages: 1-49

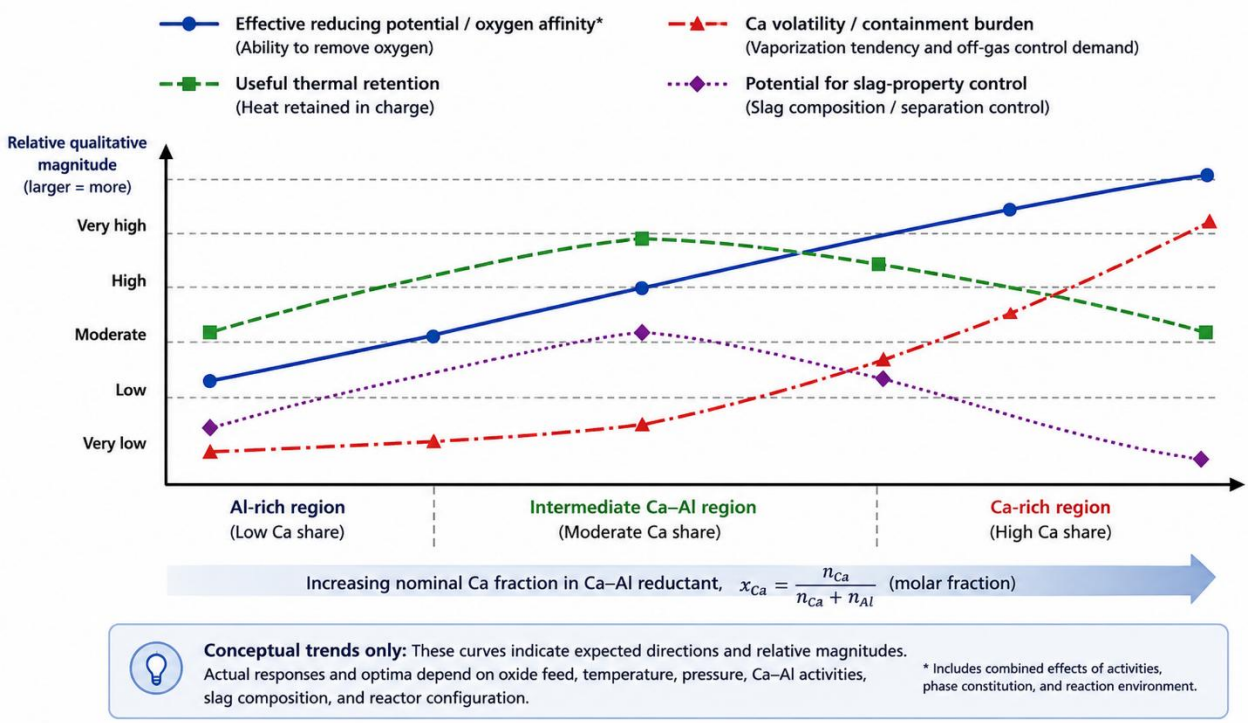


Figure 3. Conceptual effect of calcium share on coupled process responses
Note. Author's qualitative synthesis based on Fu et al. (2024), Jain and Awasthi (2025), Makrovets et al. (2022), Pikulin, Galkova, et al. (2026), Kim and Lim (2022), and Wang et al. (2020). Lines show qualitative directional tendencies only; they are not fitted experimental data, and no numerical response scale or universal optimum is implied.

Figure 3 highlights why a maximum-Ca strategy is unlikely to be optimal. Reducing strength generally increases, but the useful heat retained in the reacting condensed phase can be penalized by Ca vaporization, while slag-engineering leverage may peak at an intermediate Ca/Al ratio that produces a low-liquidus calcium-aluminate-rich melt rather than excess solid CaO.

6. Reaction Mechanisms and Kinetics

6.1 Initial contact and reaction-front formation

At the onset of heating, the mechanism depends on whether the reductant is solid, partially molten, fully molten, or partly vaporized. Fine particles improve contact area but increase oxidation sensitivity and can accelerate uncontrolled heat release. Liquid Al can penetrate porous oxide agglomerates; Ca-containing liquids may alter interfacial tension and react earlier with the most reducible or most accessible oxygen sites. Philipson et al.

CC BY

JIRRS
Journal International Review of Research Studies
Received: 02/05/2026 - **Accepted:** 26/08/2026
Vol: 01.09
DOI: 10.66104/bn5j2634
Pages: 1-49

(2024b) showed that liquid–liquid reaction phenomena are important when Al contacts calcium-silicate slag, and Deng et al. (2026) emphasized the central role of precursor state in metallothermic reaction pathways. These observations argue against treating particle size solely as a kinetic surface-area variable. Evidence status: the importance of phase state and liquid-contact phenomena in this subsection is supported primarily by Classes E and F analogues; direct Class A studies do not yet provide a general, time-resolved description of the initial reaction front across Ca–Al compositions.

6.2 Cooperative reduction and intermediate phases

The key mechanistic hypothesis for Ca–Al is cooperative rather than parallel reduction. Direct Class A evidence from the coltan and wolframite studies shows that pre-alloyed Ca–Al can generate Ca-bearing intermediates and aluminide/intermetallic participants before complete metal formation (Pikulin, Galkova, et al., 2026; Pikulin, Tyushnyakov, et al., 2026). Ca-assisted TiO_2 reduction and tantalate studies provide Classes C–D support for analogous sequential phase transformations (Cai et al., 2026; Gulyaeva, Sergeeva, et al., 2022; Gulyaeva, Udoeva, et al., 2022). The broader proposition—that Ca first transforms an oxide into a phase that is subsequently more reducible by Al, or vice versa—should therefore be treated as a system-dependent mechanistic hypothesis rather than a universal Ca–Al sequence. The implication is that the ‘stronger’ reductant may act mainly as a phase-pathway modifier in some feeds rather than performing all final oxygen removal itself.

A second possibility is that an intermetallic reductant becomes active after the initial alloy has reacted. Pikulin, Tyushnyakov, et al. (2026) identified $CaAl_2$ as a plausible subsequent reducing participant in the evolving coltan system. More generally, intermetallic formation during metallothermy is well documented in designed Cr_2Ta, $LaNi_5$, TiFe, and multicomponent alloy syntheses (Guryanov et al., 2023; Rasheed et al., 2026; Teslia et al., 2026; Yudin et al., 2024, 2025). Therefore, kinetic interpretation should track not only oxide disappearance but also transient metallic and intermetallic phases.

6.3 Rate-controlling regimes

Potential rate controls include interfacial chemical reaction, diffusion through solid product layers, liquid-phase transport through slag, migration of reductant through pores, and gas-phase Ca transport. Calciothermic powder synthesis and calcium-vapor reduction show that product porosity can preserve access to the reaction front, whereas dense intermediate layers can arrest conversion (Kasimtsev et al., 2020; Orlov & Kryzhanov, 2024; Wang et al., 2020). In liquid systems, slag viscosity and interfacial renewal can

CC BY

JIRRS
Journal International Review of Research Studies
Received: 02/05/2026 - **Accepted:** 26/08/2026
Vol: 01.09
DOI: 10.66104/bn5j2634
Pages: 1-49

become equally important. Thus, fitting a single shrinking-core or diffusion model without phase and morphology evidence can produce a mathematically adequate but physically incomplete interpretation. Evidence status: these rate-controlling regimes are supported mainly by Classes D–F and by general transport physics. Their relative importance has not been prospectively quantified across a direct Class A Ca–Al composition series, so no single kinetic model should be generalized to all mixed-reductant systems.

Figure 4 illustrates two competing pathways: direct oxygen transfer and a multistep route through Ca- or Al-bearing intermediates. The critical point is that intermediate formation is not inherently beneficial or harmful; its effect depends on morphology, continuity, melting behavior, and subsequent reducibility.

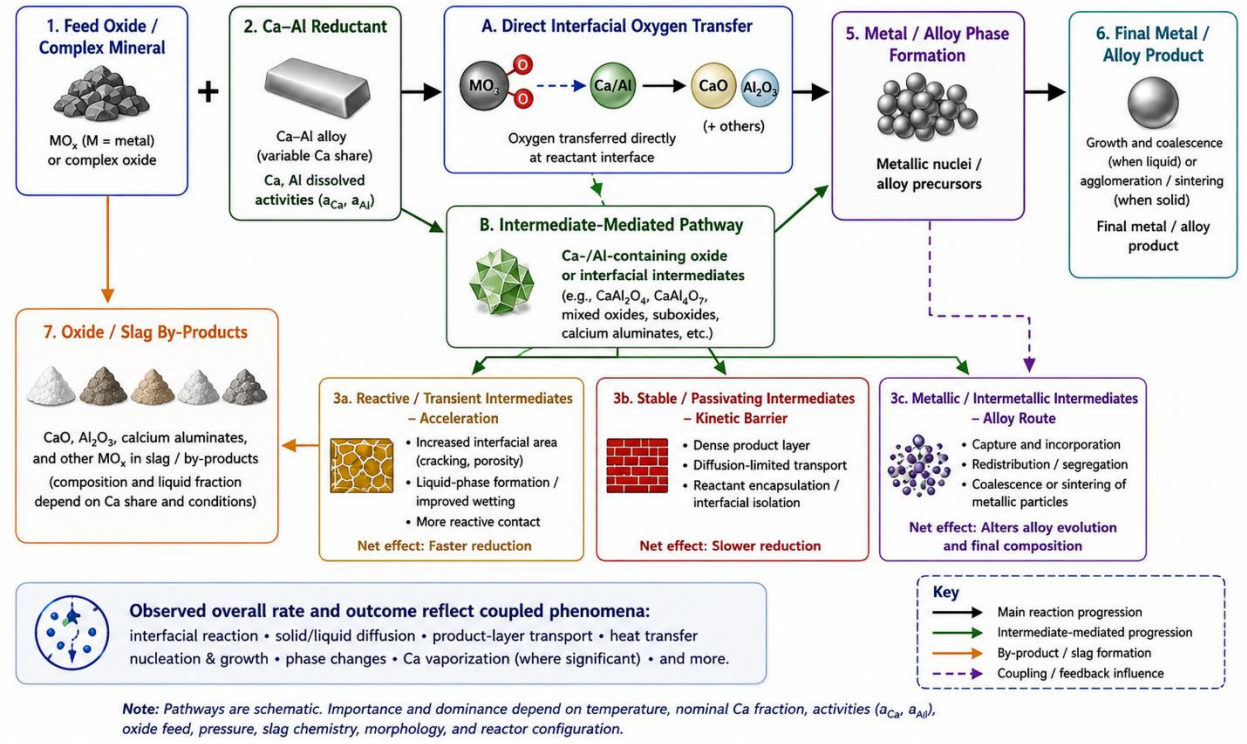


Figure 4. *Competing direct and intermediate-phase reaction pathways in Ca–Al metallothermy*
Note. Author's synthesis based on Cai et al. (2026), Deng et al. (2026), Gulyaeva, Udoeva, et al. (2022), Pikulin, Galkova, et al. (2026) and Pikulin, Tyushnyakov, et al. (2026), and Yudin et al. (2024). No graphic element was directly reproduced.

Figure 4 supports a practical experimental requirement: time-resolved XRD/SEM–EDS or interrupted-quench testing is needed whenever conversion exhibits an unexpected plateau. Without phase-resolved evidence, a plateau cannot be distinguished among

CC BY

JIRRS
Journal International Review of Research Studies
Received: 02/05/2026 - **Accepted:** 26/08/2026
Vol: 01.09
DOI: 10.66104/bn5j2634
Pages: 1-49

reductant depletion, formation of a diffusion barrier, poor slag fluidity, or loss of Ca by volatilization.

6.4 Kinetic data needed for engineering

For scale-up, kinetics should be reported in terms that close both chemistry and transport: temperature-time history, pressure, particle-size distributions, compact density, atmosphere, Ca/Al composition, mass loss, reaction extent, transient phases, and metal droplet size. The mechanistic literature on calcium hydride synthesis, Mg–Ca mediated rare-earth alloying, and aluminothermic silicon systems demonstrates the value of combining thermodynamics with kinetic or morphological observations rather than relying on final composition alone (Guryanov et al., 2023; Ren et al., 2025; Philipson et al., 2024a).

7. Phase Evolution and Product Formation

7.1 A non-universal phase sequence

A useful generic sequence is feed oxide → partially reduced oxide → Ca-bearing intermediate → Al-bearing intermediate or aluminide → metallic nuclei → alloy/intermetallic → coalesced metal + slag. This sequence is an author-developed organizing framework, not a universal mechanism. Direct Class A studies support portions of this pathway in specific coltan and wolframite systems, whereas tantalite, niobate, and cassiterite studies provide mainly Classes D–E analog evidence that complex refractory oxides can redistribute cations before metal appears (Gulyaeva, Sergeeva, et al., 2022; Gulyaeva, Udoeva, et al., 2022; Sergeeva et al., 2022; Tyushnyakov et al., 2021; Pikulin, Galkova, et al., 2026; Pikulin, Tyushnyakov, et al., 2026). Accordingly, each future mechanistic claim should state whether the relevant phase was directly observed in a pre-alloyed Ca–Al charge, observed in separately dosed/assisted systems, or inferred from an analog.

7.2 Product-phase engineering

When the intended product is an alloy, phase evolution can be designed to couple reduction and alloying. Low-oxygen Ti–48Al–2Cr–2Nb powder synthesis, WCu composite routes, electro-aluminothermic V–Ni production, and calciothermic Mo–Ti–Ta–Cr synthesis illustrate this approach (Guo et al., 2022; Cheng, K.-X. Song, Z.-W. Song, et al., 2022; Cheng, Z.-W. Song, Wang, et al., 2022; Teslia et al., 2026; Zeng et al., 2026). The advantage is that an exothermic reduction event can supply alloying heat; the disadvantage is that transient intermetallics may sequester reductant or target metal and complicate final homogenization.

CC BY

JIRRS
Journal International Review of Research Studies
Received: 02/05/2026 - **Accepted:** 26/08/2026
Vol: 01.09
DOI: 10.66104/bn5j2634
Pages: 1-49

The WCu studies are particularly useful as analogs because they link metallothermic chemistry to in situ slagging and microstructure formation. CaO addition and engineered slag formation can alter the physical separation between metallic and oxide phases, even when Ca is not the primary metallic reductant (Cheng et al., 2023, 2024). This supports a broader Ca–Al design principle: the oxide products of the reductant can be used deliberately to engineer the separation medium.

7.3 Light-element impurities and residual phases

Residual Ca, Al, O, C, N, Si, and Fe can determine whether a nominally successful reduction produces a usable metal. The calciothermic Cr–Ta literature is valuable because it explicitly examines the occurrence of light impurities and the effects of synthesis parameters on phase purity (Yudin et al., 2024, 2026). Ti deoxidation studies likewise show that Ca can modify surface oxygen and morphology (Kim & Lim, 2022; Li et al., 2020). For Ca–Al systems, the corresponding research need is a partition map showing how much Ca and Al remain in metal, slag, vapor/condensate, refractory reaction products, and unreduced feed.

Table 3 summarizes the main intermediate-phase roles that should be distinguished experimentally. This table is intentionally mechanistic; the same phase family may be beneficial in one system and detrimental in another.

Table 3. *Functional roles of intermediate phases during metallothermic reduction*

Intermediate phase family	Potential benefit	Potential penalty	Most relevant systems	Representative sources
Ca-bearing complex oxide	Destabilizes parent mineral or redistributes target cations	May become dense diffusion barrier	Tantalite/coltan/wolframite pathways	Gulyaeva, Udoeva, et al. (2022). Pikulin, Galkova, et al. (2026); Pikulin, Tyushnyakov, et al. (2026)
Calcium aluminate	Can lower effective slag liquidus and bind Al_2O_3	May crystallize if CaO/Al_2O_3 is off-window	Slag engineering	Azof et al. (2020); Huo et al. (2026)

CC BY

JIRRS
Journal International Review of Research Studies
Received: 02/05/2026 - **Accepted:** 26/08/2026
Vol: 01.09
DOI: 10.66104/bn5j2634
Pages: 1-49

Intermediate phase family	Potential benefit	Potential penalty	Most relevant systems	Representative sources
Aluminide/intermetallic	Can capture metal and assist alloy formation	May trap Al or delay final metal coalescence	Alloy/intermetallic production	Amon et al. (2024); Guo et al. (2022); Yudin et al. (2024)
Suboxide / partially reduced oxide	Provides stepwise oxygen removal	Can accumulate when reductant transport is limited	Ti/V/Nb/W systems	Cai et al. (2026); Kryzhanov & Orlov (2023); Wang et al. (2020)
Carbide or refractory-reaction phase	Occasionally useful in composite products	Usually undesirable contamination or refractory loss	Carbon-contacting systems	Khomenko et al. (2020); Yudin et al. (2026)

Note. Adapted and synthesized from the cited mechanistic and phase-analysis studies. The table does not imply that all listed phases occur in every Ca–Al system.

Table 3 shows why endpoint chemical analysis is insufficient for mechanism. Two charges with the same final metal yield may have reached that state through very different intermediate populations, and those differences can become decisive at larger scale when heat flow and diffusion distances increase.

8. Slag Engineering and Metal–Slag Separation

8.1 $CaO–Al_2O_3–MO_x$ phase relations

The strongest process-engineering argument for Ca–Al is that the reductant designs its own oxide medium. Foundational slag thermodynamics established that phase equilibria, activities, viscosity, density, and interfacial behavior—not bulk oxide percentages alone—govern metallurgical separation (Turkdogan, 1983; Verein Deutscher Eisenhüttenleute, 1995). CaO and Al_2O_3 can form calcium aluminates whose phase relations depend strongly on impurities, atmosphere, and third oxides. Experimental studies of $12CaO·7Al_2O_3$, La_2O_3-bearing slags, VO_x systems, and complex $SiO_2/Na_2O/B_2O_3$ slags demonstrate that relatively small compositional changes can shift liquidus temperature

CC BY

JIRRS
Journal International Review of Research Studies
Received: 02/05/2026 - **Accepted:** 26/08/2026
Vol: 01.09
DOI: 10.66104/bn5j2634
Pages: 1-49

and phase assemblage (Azof et al., 2020; Huo et al., 2026; Islam et al., 2022, 2024; Liu et al., 2024a, 2024b; Xie et al., 2025, 2026). Nd-bearing calcium-aluminate slag design for NdFeB recycling further illustrates how target-metal oxides can become part of the slag phase field rather than behaving as passive impurities (Blenau et al., 2023).

Mayenite-related phases are also relevant because their chemistry can accommodate substitutions and unusual electronic states. Studies of Nb substitution in mayenite and aluminothermic synthesis of mayenite-based electrides show that Ca–Al–O phases are not inert “slag only” products; they can exhibit substantial structural flexibility (Kotschote et al., 2026; Volodin et al., 2022). In reduction systems containing rare-earth, V, Nb, or other oxides, this flexibility can create sink phases that alter apparent reducibility and must be included in equilibrium and kinetic interpretations.

8.2 Viscosity, structure, wetting, and settling

Metal recovery depends on whether the slag is sufficiently fluid for droplets to move, collide, and coalesce. CaO/Al_2O_3 ratio, MgO, SiO_2, B_2O_3, Fe_tO, Cr_2O_3, and other network-modifying or network-forming oxides affect melt structure and transport properties. Molecular-dynamics and experimental studies confirm strong composition–viscosity coupling in $CaO–Al_2O_3$-based systems (Kim & Park, 2020; Ma et al., 2025; Yuan et al., 2022; X. Zhang et al., 2022; L. Zhang et al., 2022). Thermal-property measurements of calcium-aluminate materials provide additional context for the heat-transfer side of slag behavior (Kulu et al., 2021). Fluxed-slag design calculations for manganese aluminothermy also show that deliberately modifying the oxide phase assemblage can recover aluminum value while changing the thermochemical path (Coetsee & De Bruin, 2026).

Interfacial phenomena can be equally decisive. C. Wang et al. (2025) quantified wetting and spreading between refractories and molten calcium-aluminate slags, while G. Wang et al. (2025) examined dissolution kinetics of calcium-aluminate inclusions in steelmaking slags. These studies are not direct Ca–Al metallothermy, but they demonstrate that contact angles, dissolution rates, and slag/refractory interactions evolve dynamically. Pereira (2026) further emphasizes that droplet coalescence and physical entrainment must be separated conceptually from chemical dissolution when evaluating metal losses.

8.3 Separation as a coupled design target

Figure 5 shows the coupling among the Ca/Al ratio, oxide products, slag phase field, physical properties, and final metal recovery. The same reductant variable that drives

CC BY

JIRRS
Journal International Review of Research Studies
Received: 02/05/2026 - **Accepted:** 26/08/2026
Vol: 01.09
DOI: 10.66104/bn5j2634
Pages: 1-49

oxygen removal therefore changes the medium through which the reduced metal must separate.

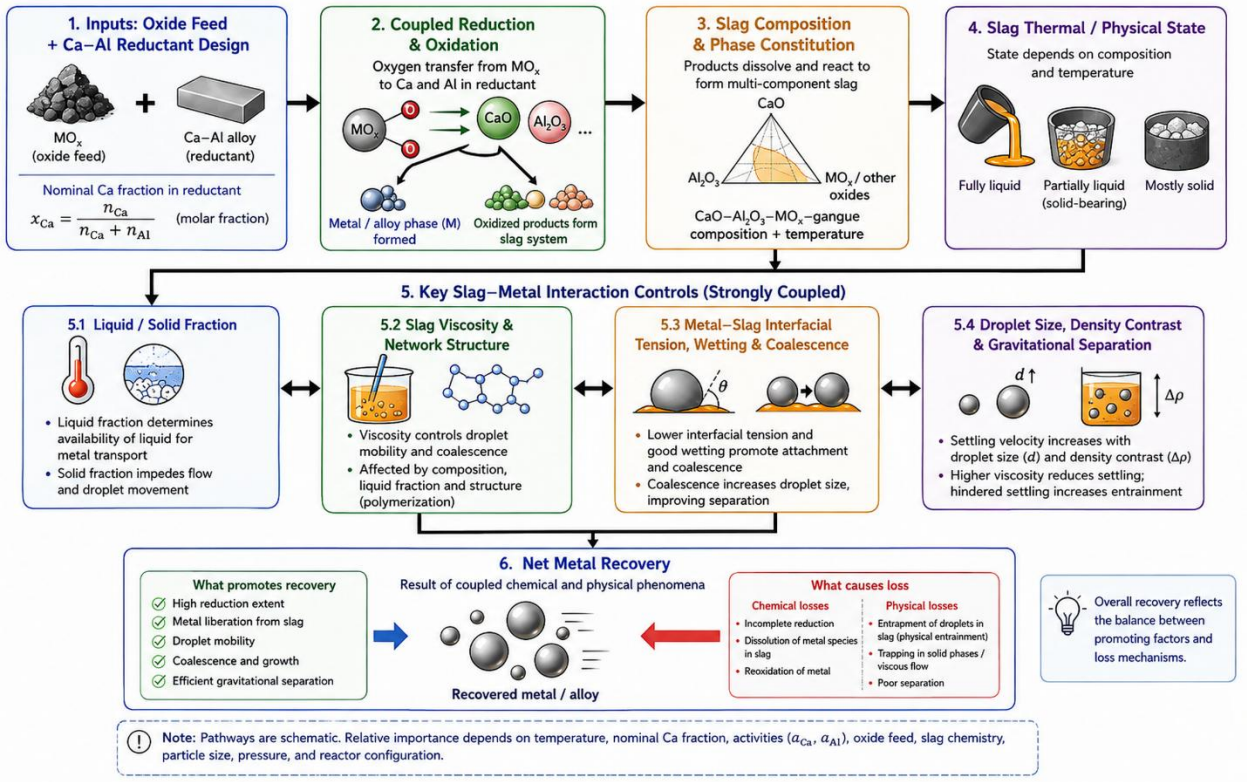


Figure 5. *Coupled slag engineering and metal-recovery pathway in Ca–Al metallothermy*
Note. Author's synthesis based on Cheng et al. (2024), Kim and Park (2020), Ma et al. (2025), Pereira (2026), Song et al. (2021), C. Wang et al. (2025), and X. Zhang et al. (2022). No graphic element was directly reproduced.

Figure 5 explains a frequently overlooked source of non-monotonic performance. Adding Ca can improve thermodynamic reduction but can simultaneously increase the solid fraction if the resulting CaO is not incorporated into a low-liquidus calcium aluminate or multicomponent slag. In that case, chemical conversion rises while metal settling worsens. The opposite can occur if the added Ca shifts the slag toward a fluid-phase field and promotes droplet coalescence.

Separation-time studies for aluminothermic silicon and for metal–slag separation for TiAl and CuW provide practical analogues of this behavior (Bullón et al., 2025; Cheng et al., 2024; Song et al., 2021). Pilot-scale silicon alloy production further demonstrates that slag composition and separation remain important as the process moves beyond laboratory batches (Zhu et al., 2024).

CC BY

JIRRS
Journal International Review of Research Studies
Received: 02/05/2026 - **Accepted:** 26/08/2026
Vol: 01.09
DOI: 10.66104/bn5j2634
Pages: 1-49

Table 4 summarizes the key slag variables to be reported in Ca–Al studies. Their omission makes it impossible to decide whether a low metal yield reflects incomplete reduction or physical retention of already reduced metal.

Table 4. *Slag and interfacial variables controlling metal–slag separation*

Variable	Primary physicochemical role	Engineering consequence / measurement	Representative sources	Interpretive direction / usable process window
CaO/Al_2O_3 ratio	Controls calcium-aluminate phase field and polymerization	Liquidus, solid fraction, viscosity	Azof et al. (2020); X. Zhang et al. (2022)	Prefer a liquidus below the intended process temperature and a low residual solid fraction; no universal CaO/Al_2O_3 ratio is implied.
Third oxides: SiO_2, MgO, B_2O_3, Na_2O	Shift liquidus and melt structure	Viscosity, phase stability, refractory interaction	Islam et al. (2022, 2024); Ma et al. (2025)	Use third oxides only where they shift the real slag toward a sufficiently liquid, low-to-moderate-viscosity field without unacceptable refractory attack.
Transition-metal oxides: Fe_tO, VO_x, Cr_2O_3	Participate in redox and network structure	Residual reducible oxide, viscosity, phase partitioning	Kim & Park (2020); Liu et al. (2024a); Yuan et al. (2022)	Minimize persistent reducible/solid oxide phases consistent with the target redox state; interpret chemistry together with phase fraction.
Interfacial wetting	Controls adherence to refractory and metal-droplet behavior	Contact angle, spreading time	C. Wang et al. (2025)	Favor interfacial conditions that permit metal-droplet detachment/coalescence and limit persistent slag films on metal; contact-angle targets are system-specific.
Droplet population	Controls gravitational/forced separation	Size distribution, coalescence, entrainment	Pereira (2026); Song et al. (2021)	Favor growth/coalescence of recoverable droplets and a low entrained-fines fraction; report the full size distribution rather than the mean alone.
Thermal state	Determines liquid fraction and settling time	Temperature-time history, superheat	Bullón et al. (2025); Kulu et al. (2021)	Maintain sufficient superheat and liquid residence time for settling/coalescence without excessive Ca volatilization or refractory dissolution.
Metal–slag density contrast / settling	Provides gravitational or forced-separation driving force	High-temperature densities or validated proxies; settling velocity/residence time	Bullón et al. (2025); Song et al. (2021)	Seek sufficient density contrast and residence time to promote separation; required values depend on droplet size, viscosity, and hydrodynamics.

Note. Adapted and synthesized from the cited slag, interfacial, and separation literature.

Table 4 therefore moves from a reporting checklist toward an interpretive process window. Desirable directions are a liquidus below the operating temperature, low residual solid fraction, sufficient density contrast, low-to-moderate viscosity compatible with droplet

CC BY

JIRRS
Journal International Review of Research Studies
Received: 02/05/2026 - **Accepted:** 26/08/2026
Vol: 01.09
DOI: 10.66104/bn5j2634
Pages: 1-49

motion, interfacial conditions favorable to droplet detachment and coalescence, and limited refractory dissolution. Universal numerical thresholds are deliberately not proposed because they depend on metal density, droplet size, slag chemistry, pressure, and reactor hydrodynamics. At minimum, studies should report slag bulk composition, identified crystalline and liquid phases, temperature–time profile, viscosity or a validated proxy, density or settling proxy, wetting/contact-angle information where feasible, metal droplet size distribution, and target metal retained in final slag.

9. Process Variables and the Operating Window

9.1 Feed, reductant, and charge preparation

Feed mineralogy, reducible oxygen, particle size, moisture, impurity oxides, and physical mixing determine the initial contact topology. Fine grinding may accelerate reaction but can also promote oxidation of Ca–Al particles and produce an excessively fast thermal event. Briquetting or compaction improves contact but can reduce gas permeability, which matters if Ca vapor or gaseous products must move through the bed. The importance of precursor state in metallothermic kinetics and of industrial retort charge conditions in aluminothermic Mg production demonstrates that charge architecture is an engineering variable, not merely sample preparation (Deng et al., 2026; Fu et al., 2024).

9.2 Ca/Al ratio, dosage, temperature, and pressure

The Ca/Al ratio should be reported in at least three forms: alloy composition, molar Ca/Al, and χCa. Total dosage should additionally be expressed through R_eq. These descriptors separate two decisions that are often conflated: how much reducing capacity is supplied and how that capacity is divided between Ca and Al. A charge can therefore be Ca-rich but reductant-deficient, or Al-rich but strongly over-stoichiometric. Pressure and temperature then determine how much of the nominal Ca remains available in the condensed reaction zone.

Figure 6 presents the preferred process region as an operating window rather than a single optimum. At low reducing/thermal intensity, conversion and slag melting may be incomplete. At excessively Ca-rich or severe conditions, volatilization, refractory attack, pressure excursions, and loss of controllability can dominate.

CC BY

JIRRS
Journal International Review of Research Studies
Received: 02/05/2026 - **Accepted:** 26/08/2026
Vol: 01.09
DOI: 10.66104/bn5j2634
Pages: 1-49



Figure 6. *Conceptual operating window for Ca–Al metallothermic reduction*
Note. Author's synthesis based on Fu et al. (2024), Makrovets et al. (2022), Kim and Lim (2022), Pikulin, Galkova, et al. (2026), and Wang et al. (2020). Boundaries are qualitative and system-specific; no graphic element was directly reproduced.

Figure 6 also emphasizes that the window moves. A slag flux that lowers the liquidus, a finer feed, preheating, vacuum, an inert-gas pressure, or a more insulating reactor can all shift the Ca/Al ratio required to achieve the same conversion and separation. Process development should therefore map a multivariable domain rather than optimize one factor at a time.

Table 5 presents the minimum set of operating variables and responses required to compare Ca–Al experiments across laboratories. The intent is to convert descriptive thermite experiments into datasets suitable for mechanistic and scale-up analysis.

Table 5. *Recommended reporting matrix for Ca–Al metallothermic experiments*

Variable group	Minimum reported quantities	Why it matters
Feed	Mineralogy; oxide assay; reducible O; impurity oxides; particle-size distribution	Phase pathway and stoichiometric oxygen demand

CC BY

JIRRS
Journal International Review of Research Studies
Received: 02/05/2026 - **Accepted:** 26/08/2026
Vol: 01.09
DOI: 10.66104/bn5j2634
Pages: 1-49

Variable group	Minimum reported quantities	Why it matters
Ca–Al reductant	wt.% Ca/Al; phases; particle size; oxidation state	Activities, ignition/contact behavior
Reductant dosage	R_eq; absolute g or mol per kg feed	Under/over-stoichiometry
Ca contribution	Molar Ca/Al; χCa	Partition of oxygen-removal capacity
Charge architecture	Mixing index; density; porosity; briquette dimensions	Heat/mass transfer and vapor transport
Thermal conditions	Preheat; peak T; T–t curve; heat loss estimate	Reaction completion and slag liquid fraction
Atmosphere	Gas type; pressure; vacuum level; leak rate	Ca retention/vapor transport and oxidation control
Slag state	Composition; liquidus; phase fraction; viscosity/proxy	Coalescence and settling
Products	Metal yield; recovery; O/Al/Ca/C/N/Fe/Si; slag metal loss	Quality and mass-balance closure

Note. Author's synthesis informed by the experimental variables emphasized across Deng et al. (2026), Fu et al. (2024), Lee et al. (2024), Pikulin, Galkova, et al. (2026) and Pikulin, Tyushnyakov, et al. (2026), and Zhu et al. (2024).

Table 5 is deliberately more demanding than conventional thermite reporting. The additional measurements are justified because Ca introduces a volatile component and because the resulting slag can change substantially with reductant composition. A mass loss that is ignored in an Al-only system may correspond to a significant Ca balance error in a Ca–Al process.

10. Reactor Design, Process Control, and Safety

10.1 Reactor configurations

Potential reactor configurations include refractory-lined metallothermic vessels, sealed retorts, shaft-type reactors, induction-assisted vessels, self-propagating high-temperature synthesis reactors, and gravity- or centrifugal-assisted systems. The correct choice depends on whether the reaction must be self-heating, externally heated, pressure

CC BY

JIRRS
Journal International Review of Research Studies
Received: 02/05/2026 - **Accepted:** 26/08/2026
Vol: 01.09
DOI: 10.66104/bn5j2634
Pages: 1-49

controlled, or operated under vacuum. Industrial aluminothermic Mg retorts and pilot-scale aluminothermic Si alloy production provide scale-relevant baselines for thermal integration and batch handling, while induction metallothermy illustrates the benefit of externally controllable heat for complex alloy feeds (Fu et al., 2024; Makhambetov et al., 2026; Zhu et al., 2024).

10.2 Atmosphere, Ca-vapor management, and instrumentation

A Ca–Al reactor should be treated as a reactive vapor system whenever the operating temperature approaches conditions at which Ca vapor pressure is significant. Inert gas or vacuum control, pressure measurement, sealed charging, off-gas condensation, filtration, and relief capacity should therefore be integrated into the flowsheet rather than added after reaction testing. Calcium-vapor reductions and Ca-based Ti deoxidation confirm that reactive Ca species can travel beyond the original condensed contact zone (Kim & Lim, 2022; Kryzhanov & Orlov, 2023; Wang et al., 2020).

Temperature measurement should combine embedded thermocouples where survivable with optical pyrometry or infrared methods for fast exothermic events. A single post-test furnace setpoint is not an adequate thermal descriptor. If the process is self-propagating, the local peak temperature can exceed the nominal furnace temperature substantially; if Ca evaporates, latent heat and vapor transport can also distort the simple adiabatic picture.

10.3 Refractory compatibility and contamination

Refractory selection is unusually important because Ca can reduce or infiltrate oxide refractories and can react with carbon-containing materials. Wetting data for calcium-aluminate slags show that refractory interactions depend on both chemistry and time (C. Wang et al., 2025). Carbon contact also raises the possibility of carbide formation or carbon pickup, an issue relevant to refractory intermetallic and Cr–Ta systems, where light-element impurities can persist in the product (Khomenko et al., 2020; Yudin et al., 2026). The design objective is therefore not simply high-temperature resistance but chemical compatibility with both reductant and slag.

Figure 7 shows a conceptual process arrangement that separates protected Ca–Al handling, reaction, Ca-vapor/off-gas control, metal recovery, slag conditioning, and downstream refining. The flowsheet is generic and should be adapted to the volatility and product form of the target system.

CC BY

JIRRS
Journal International Review of Research Studies
Received: 02/05/2026 - **Accepted:** 26/08/2026
Vol: 01.09
DOI: 10.66104/bn5j2634
Pages: 1-49

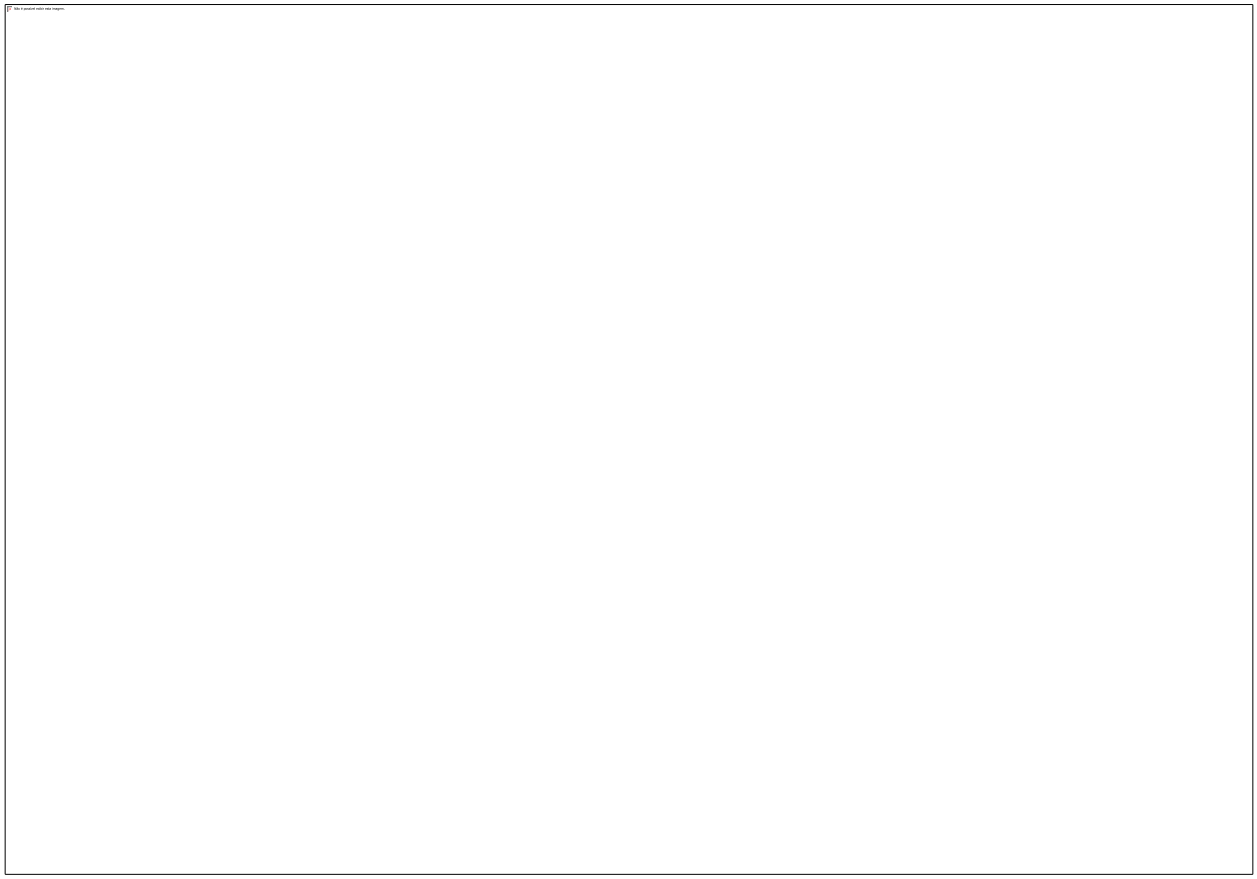


Figure 7. *Conceptual reactor and auxiliary system for Ca–Al metallothermy*
Note. Author's engineering synthesis based on Fu et al. (2024), Kim and Lim (2022), Kryzhanov and Orlov (2023), Gorkunov and Munter (2007), and Zhu et al. (2024). Metal recovery/refining and slag conditioning are represented as separate downstream branches; no graphic element was directly reproduced.

Figure 7 makes two scale-up requirements explicit. First, Ca-bearing feed handling must exclude water and minimize uncontrolled oxidation. Second, vapor/pressure management is part of the reaction system itself. A reactor that produces excellent small-batch conversion in an open crucible may not be transferable to a sealed industrial unit unless Ca transport and condensation are characterized.

10.4 Safety envelope

The main hazards are Ca reactivity with moisture, oxidation and ignition of fine metallic powders, rapid aluminothermic heat release, Ca vapor generation, molten-product ejection, overpressure, refractory failure, and reactive residues. These hazards can interact: moisture ingress can generate gas and heat rapidly, an overly fine charge can

CC BY

JIRRS
Journal International Review of Research Studies
Received: 02/05/2026 - **Accepted:** 26/08/2026
Vol: 01.09
DOI: 10.66104/bn5j2634
Pages: 1-49

accelerate ignition, and high Ca activity can increase both reduction rate and vapor load. Safety therefore favors controlled particle-size specifications, inert storage and charging, ignition interlocks, pressure relief, remote operation, containment of molten discharge, and validated residue-passivation procedures. These recommendations are consistent with combustible-metal hazard-control principles in NFPA 484 (National Fire Protection Association, 2022). Environmental and safety claims should not be inferred from stoichiometry alone; they require a complete process inventory and a site-specific process hazard analysis. For scale-up, these controls are not optional design features but validation gates: no Ca–Al route should be considered scalable until inert handling and moisture exclusion, pressure relief, Ca-vapor/condensate management, refractory compatibility, molten-product containment, and residue passivation have been demonstrated at the relevant pilot scale.

11. Performance, Product Purity, Environmental and Economic Considerations

11.1 Distinguishing conversion, yield, and recovery

Three metrics should be reported separately. Oxide conversion measures the fraction of the target oxide that is chemically transformed. Metal yield measures recovered metal mass relative to the theoretical metal in the feed. Metal recovery measures the distribution of the target metal between the collected metallic product and slag, dust, condensate, and unreduced residue. These quantities are not interchangeable: high conversion can coexist with poor recovery when already reduced metal remains as fine droplets, intermetallic fragments, or physically entrained particles in slag (Cheng et al., 2024; Pereira, 2026; Song et al., 2021). Consequently, a Ca–Al study should report chemical conversion and phase-distribution recovery independently whenever possible; otherwise, a single ‘yield’ value can conceal whether the governing loss is thermodynamic/kinetic or physical separation.

11.2 Product purity and reductant-derived impurities

Residual Al and Ca should be treated differently. Aluminum can remain dissolved or form stable aluminides, which may be desirable for TiAl or Al–Ce products but unacceptable in high-purity refractory metals. Calcium may be easier to remove by evaporation or slag partitioning in some systems, but only if the product and operating pressure permit it. Deoxidation and calciothermic studies on Ti, Nb/Ta, rare-earth metals, and intermetallics show that final oxygen and light-element contents depend on both reaction conditions and post-reaction treatment (Kim & Lim, 2022; Orlov & Kryzhanov, 2024; Sahoo et al., 2024; Yudin et al., 2025, 2026).

CC BY

JIRRS
Journal International Review of Research Studies
Received: 02/05/2026 - **Accepted:** 26/08/2026
Vol: 01.09
DOI: 10.66104/bn5j2634
Pages: 1-49

Secondary refining can therefore be an integral part of a Ca–Al flowsheet. Slag treatment of Si–Ca–Al alloys, remelting Ti scrap with Ca and halide fluxes, and recycling of metallothermic or calciothermic slags illustrate routes for separating or recovering residual value after the main reduction event (Emil-Kaya et al., 2024; Huang et al., 2025; Su et al., 2026).

11.3 Slag valorization and environmental performance

Ca–Al slags should not automatically be classified as inert waste. Calcium-aluminate-rich residues may be candidates for hydrometallurgical recovery, alumina production, carbonation, construction-related uses, or targeted recovery of residual rare earths and radioactive elements, depending on composition and hazard status. Examples include recovery of rare earths from calciothermic slag, leaching of aluminothermic slag for U/Th, alumina recovery from SisAl slags, and carbonation/leaching behavior of calcium-aluminate-bearing monoliths (Huang et al., 2025; Moura et al., 2022; Usta et al., 2023; Zhu & Safarian, 2023). The production of Al–Si–Ca alloys from secondary Si and fluoride-bearing residues further demonstrates that Ca–Al-bearing material cycles can be linked to broader circular raw-material strategies (Ming et al., 2025).

Life-cycle performance is similarly system-specific. Aluminothermic silicon has been examined in the context of industrial symbiosis and carbon-neutrality claims, showing that electricity source, aluminum supply, coproduct credits, and slag valorization strongly affect the result (Pastor-Vallés et al., 2025). A Ca–Al route adds burdens for calcium production and handling but may offset them through higher recovery, reduced downstream refining, or a more valuable slag. Environmental comparison must therefore be based on a consistent functional unit, such as kilograms of on-spec metal, rather than kilograms of reductant. This review does not establish environmental superiority of Ca–Al routes. It identifies inventory terms and boundary conditions that future LCA should evaluate on a consistent functional unit, preferably kilograms of on-spec metal at the stated recovery and purity.

11.4 Economic logic

The economic question is whether additional Ca and containment costs are offset by higher conversion/recovery, lower Al contamination, easier refining, or better slag handling. A screening cost function should include reductant, energy/preheat, inert gas or vacuum, reactor/refractory consumption, off-gas treatment, refining, slag handling, yield loss, and coproduct credits (Karati et al., 2025; Palumbo & Chubukov, 2023). No TEA is claimed here; Table 6 identifies variables that a future plant-specific assessment should quantify on an on-spec-metal basis. Accordingly, the review also does not establish

CC BY

JIRRS
Journal International Review of Research Studies
Received: 02/05/2026 - **Accepted:** 26/08/2026
Vol: 01.09
DOI: 10.66104/bn5j2634
Pages: 1-49

economic superiority of Ca–Al. It proposes the minimum variables required for future plant-specific TEA, including sensitivity to reductant price, Ca loss, yield, refractory life, off-gas treatment, refining burden, and coproduct or slag credits.

Table 6 provides a decision-oriented comparison of Ca, Al, and Ca–Al. The mixed reductant should be selected only when its tunability yields a measurable process advantage that outweighs the additional complexity.

Table 6. *Decision-oriented comparison of calcium, aluminum, and Ca–Al reductants*

Criterion	Calcium	Aluminum	Ca–Al alloy
Nominal reducing strength / oxygen affinity	Generally very high; oxide dependent	High; oxide dependent	Activity-, composition-, and phase-dependent
Volatility burden	High	Low	Intermediate to high; pressure dependent
Self-heating potential	System dependent	Generally strong	Adjustable, but Ca vaporization can consume heat
Oxide product	CaO-rich	Al_2O_3-rich	CaO–Al_2O_3 / calcium-aluminate-rich
Slag-engineering leverage	Limited alone	Aluminous slag may be refractory	Potentially high if CaO/Al_2O_3 enters fluid phase field
Residual reductant impurity	Ca often removable in suitable systems	Al may remain dissolved/intermetallic	Can reduce Al burden but introduces Ca-control requirement
Process control	High reactivity and vapor sensitivity	Most established	More complex but more tunable
Best-fit application	Very stable oxides; deoxidation; powders	Conventional thermite and alloying	Complex oxides where phase/slag/purity benefits justify complexity

Note. Author's critical synthesis based on Athelli and Reddy (2026), Makrovets et al. (2022), Nababan et al. (2026), Palumbo and Chubukov (2023), and Rafique (2024).

CC BY

JIRRS
Journal International Review of Research Studies
Received: 02/05/2026 - **Accepted:** 26/08/2026
Vol: 01.09
DOI: 10.66104/bn5j2634
Pages: 1-49

Table 6 is a screening framework, not a universal ranking or TEA. Ca–Al is most compelling when coupled benefits occur, such as stronger reduction plus lower residual Al or improved reduction plus a more separable slag. If the only benefit is a modest Gibbs-energy advantage, pure Ca or modified aluminothermy may be simpler.

12. Scale-Up and Comparative Synthesis

12.1 Why geometric scale-up is inadequate

Metallothermic scale-up is not achieved by preserving reagent percentages while increasing vessel volume: heat loss, Ca vapor transport, slag depth, mixing uniformity, and refractory interaction all change. Direct scale-relevant evidence exists for calcium–aluminothermal Nb_2O_5 reduction, with Gorkunov and Munter (2007) reporting pilot- and full-scale operations and industrial ingots up to ~2000 kg. Contemporary Ca–Al-specific scale-up evidence is sparse; aluminothermic Si pilot work and industrial Mg retorts are therefore used only as thermal/transport analogs (Fu et al., 2024; Zhu et al., 2024). Ca–Al scale-up additionally requires closure of Ca across metal, slag, vapor/condensate, refractory products, and dust.

12.2 Required closure for pilot validation

A credible pilot campaign should close target-metal, O, Ca, Al, slag-former, and off-gas/condensable-Ca balances while separately monitoring refractory integrity, thermal history, metal-droplet/button formation, and slag liquid fraction. Historical Nb practice supports balance-based scale validation (Gorkunov & Munter, 2007); contemporary analog systems support transient thermal and separation similarity (Fu et al., 2024; Zhu et al., 2024). This distinction between conserved material-balance terms, equipment-condition monitoring, demonstrated Ca + Al practice, and analog-based inference is maintained here.

Figure 8 outlines the progression from thermochemical screening to industrial deployment, with each stage adding a new transport or reliability constraint rather than simply increasing batch size.

CC BY

JIRRS
Journal International Review of Research Studies
Received: 02/05/2026 - **Accepted:** 26/08/2026
Vol: 01.09
DOI: 10.66104/bn5j2634
Pages: 1-49

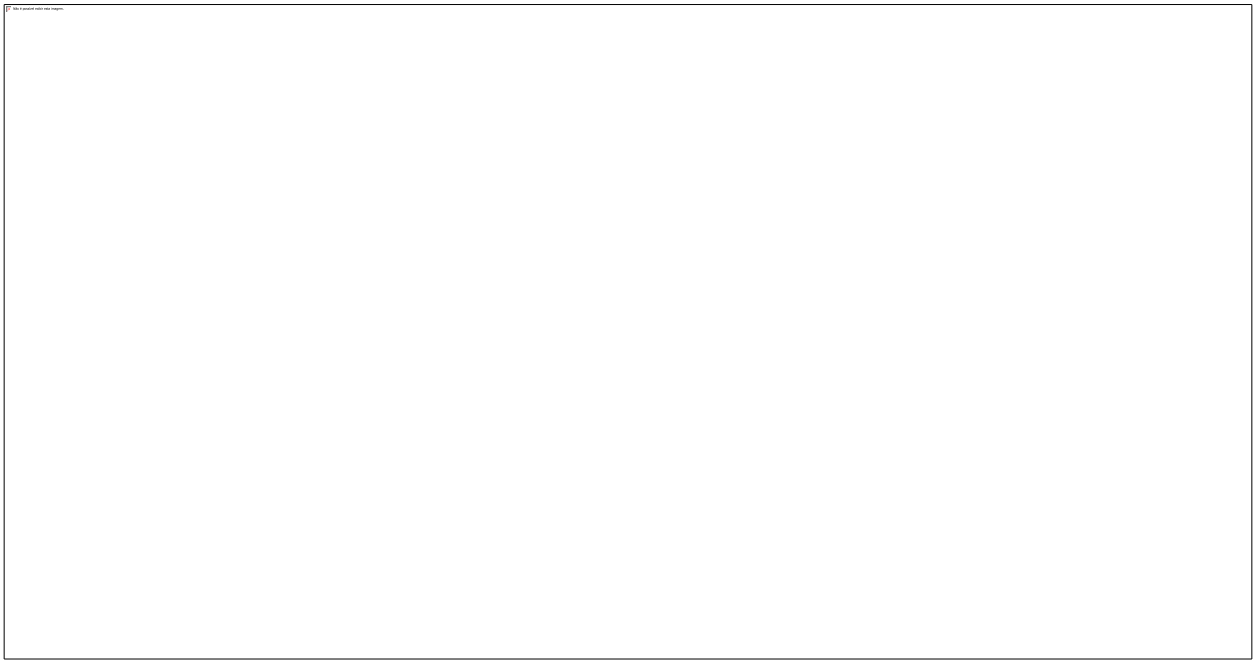


Figure 8. *Laboratory-to-industrial scale-up logic for Ca–Al metallothermy*
Note. Author's engineering synthesis based on Gorkunov and Munter (2007), Deng et al. (2026), Fu et al. (2024), and Zhu et al. (2024). Material-balance closure is shown separately from refractory-integrity monitoring; direct Ca + Al scale evidence and aluminothermic analogues are distinguished in the accompanying text. No graphic element was directly reproduced.

Figure 8 identifies the key scale-up invariant: the process should preserve the coupled heat–mass-transfer–phase-separation regime that produced the favorable laboratory result. If the laboratory success depended on rapid heat release followed by a long liquid-settling period, an industrial reactor must reproduce both features, not merely the same Ca/Al ratio.

12.3 Validation status of the scale-up framework

The laboratory-to-industrial sequence in Figure 8 is an author-developed engineering logic, not an empirically validated scale-up protocol. Prospective validation is required across at least two chemically distinct Ca–Al systems before the framework can be treated as transferable. A successful pilot should demonstrate not only material-balance closure and product quality but also reproducible thermal history, Ca-vapor/condensate behavior, slag liquid fraction and settling, refractory compatibility, and the safety gates defined in Section 10.4. Until such validation exists, the framework should be used as a

CC BY

JIRRS
Journal International Review of Research Studies
Received: 02/05/2026 - **Accepted:** 26/08/2026
Vol: 01.09
DOI: 10.66104/bn5j2634
Pages: 1-49

checklist for experimental design and scale-up risk reduction rather than as a predictive scale-up law.

12.4 Comparative synthesis across the literature

The literature collectively supports five conclusions. First, precursor and phase pathway strongly influence metallothermic performance, as shown across Ti, Nb/Ta, W, and rare-earth systems (Cai et al., 2026; Deng et al., 2026; Gulyaeva, Udoeva, et al., 2022; Pikulin, Galkova, et al., 2026; Pikulin, Tyushnyakov, et al., 2026). Second, Ca can operate through both condensed and vapor pathways, so pressure is a chemical variable rather than solely a safety variable (Kim & Lim, 2022; Kryzhanov & Orlov, 2023; Wang et al., 2020). Third, $CaO–Al_2O_3$ phase chemistry is sufficiently flexible that slag design can either enhance or obstruct recovery (Azof et al., 2020; Ma et al., 2025; Xie et al., 2026). Fourth, physical metal–slag separation can control practical yield independently of chemical conversion (Bullón et al., 2025; Cheng et al., 2024; Pereira, 2026; Song et al., 2021). Fifth, no single reductant is universally best; route selection must include product purity, containment, slag, downstream refining, and feed-specific strategic context (Nababan et al., 2026; Ortega et al., 2026; Palumbo & Chubukov, 2023; Rafique, 2024; Sohn, 2026).

13. Knowledge Gaps and Conclusions

13.1 Knowledge gaps and research priorities

The dominant gap is the lack of activity-based reporting. Most applied studies report alloy composition but not aCa or aAl, even though the thermodynamic state of the reductant depends on phase and temperature. CALPHAD-informed descriptions should therefore be linked to measured phase constitution and pressure. This is particularly important for systems in which Ca vapor participates or calcium aluminates sequester oxide components (Makrovets et al., 2022; Wang et al., 2026; Zhi et al., 2022).

A second gap is incomplete reaction-pathway resolution. Recent in situ and phase-transformation studies show that intermediates can be decisive, yet systematic interrupted-reaction datasets remain scarce (Deng et al., 2026; Gulyaeva, Udoeva, et al., 2022; Pikulin, Galkova, et al., 2026; Pikulin, Tyushnyakov, et al., 2026). Future studies should combine time-resolved diffraction, microscopy, local chemical analysis, and mass-loss monitoring to distinguish reaction-front chemistry from post-reaction cooling transformations.

A third gap is inadequate coupling between slag science and metal recovery. $CaO–Al_2O_3–MO_x$ phase-equilibrium data are expanding, but viscosity, density, interfacial tension,

CC BY

JIRRS
Journal International Review of Research Studies
Received: 02/05/2026 - **Accepted:** 26/08/2026
Vol: 01.09
DOI: 10.66104/bn5j2634
Pages: 1-49

wetting, and droplet-size data for real metallothermic slags remain sparse (Ma et al., 2025; C. Wang et al., 2025; Xie et al., 2025, 2026). The most useful future experiments will measure chemical conversion and physical entrainment in the same test.

A fourth gap concerns process closure and contemporary scale-up evidence. Historical Nb production shows that mixed Ca + Al operation can be industrially feasible in a specific system (Gorkunov & Munter, 2007), but modern Ca–Al master-alloy studies rarely report complete Ca/Al balances, condensate inventories, refractory changes, and metal physically retained in slag. Modern scale data are richer for aluminothermic analogues (Fu et al., 2024; Zhu et al., 2024). Future models should couple CALPHAD with transient heat transfer, kinetics, and CFD-based droplet/separation analysis rather than treat the reactor as an equilibrium black box.

Table 7 prioritizes the research program needed to move Ca–Al metallothermy from promising mechanistic observations toward a reproducible engineering platform.

Table 7. *Priority knowledge gaps and research directions for Ca–Al metallothermy*

Priority	Gap	Current limitation	Recommended research action	Expected engineering value
1	Metallic activities	Few studies report aCa and aAl	CALPHAD + alloy phase analysis + vapor-pressure measurements	Reliable reductant design
2	Reaction pathway	Intermediate phases often inferred only from final products	Interrupted/quench tests; in situ XRD where feasible	Mechanistic control and kinetic models
3	Ca-vapor role	Loss versus beneficial transport rarely separated	Closed-reactor Ca balance and condensate mapping	Pressure and reactor design
4	Slag transport properties	Real CaO–Al_2O_3–MO_x viscosity/wetting data sparse	High-T viscosity, density, contact angle and phase-fraction data	Predictable metal separation
5	Metal entrainment	Chemical and physical losses commonly merged	Droplet sizing + slag digestion/mass balance	True recovery optimization

CC BY

JIRRS
Journal International Review of Research Studies
Received: 02/05/2026 - **Accepted:** 26/08/2026
Vol: 01.09
DOI: 10.66104/bn5j2634
Pages: 1-49

Priority	Gap	Current limitation	Recommended research action	Expected engineering value
6	Refractory compatibility	Ca attack and carbon pickup insufficiently quantified	Static/dynamic corrosion tests under reaction atmosphere	Longer campaign life and purity
7	Scale-up criteria	Reagent ratio often scaled without transport similarity	Pilot heat/mass balance, off-gas, settling and refractory monitoring	Industrial transferability
8	Economics and circularity	Few Ca vs Al vs Ca–Al comparisons on on-spec metal basis	TEA + LCA with slag/condensate valorization credits	Defensible route selection

Note. Author's critical synthesis informed by gaps identified across the 2007 foundational study and the 2020–2026 contemporary corpus.

Table 7 indicates that the next advances are unlikely to come from simply testing more Ca/Al ratios. The highest-value work is integrative: thermodynamic activity, transient phases, Ca volatility, slag transport, droplet behavior, refractory interaction, and process economics must be resolved in the same experimental framework.

13.2 Limitations of the Review and Evidence Base

This review has eight principal limitations. First, direct pre-alloyed Ca–Al evidence is sparse: only three Class A studies provide the highest-weight alloy-specific evidence, so broad mechanistic or performance claims necessarily rely on bounded analogues. Second, the search was structured but narrative; database-level retrieval counts, duplicate-removal counts, and exclusion logs were not retained, so corpus completeness cannot be independently reconstructed as it could in a PRISMA-compliant systematic review. Third, evidence classes were assigned by the sole author as single-reviewer interpretive coding; no independent second coder or inter-rater reliability coefficient is available. Supplementary Table S1 improves auditability but does not substitute for independent reliability testing.

Fourth, much of the activity, volatility, kinetic, and slag-property interpretation derives from Classes B–F rather than direct Class A evidence, and transferability is therefore system-specific. Fifth, Ca and Al activities, complete Ca vapor/condensate inventories, and closed Ca/Al/O/refractory balances are missing from many primary studies. Sixth, R_{eq} and χCa

CC BY

JIRRS
Journal International Review of Research Studies
Received: 02/05/2026 - **Accepted:** 26/08/2026
Vol: 01.09
DOI: 10.66104/bn5j2634
Pages: 1-49

are stoichiometric normalization descriptors only, while A–T–P–S–Q and the scale-up sequence are author-developed interpretive tools; none has been validated as a quantitative predictor of recovery or as an industrial protocol. Seventh, contemporary pilot validation of pre-alloyed Ca–Al routes is largely absent, with historical Nb practice and modern aluminothermic systems providing only bounded scale analogies. Eighth, no formal TEA or LCA was performed; economic and environmental comparisons remain conditional and must be tested on an on-spec-metal functional unit.

13.3 Conclusions

Ca–Al metallothermy is best understood as an engineered hybrid between calciothermy and aluminothermy, but the available evidence does not support treating it as the linear sum of the two or as a generally superior route. Direct pre-alloyed evidence remains sparse, so alloy-specific claims must stay separated from conclusions inferred from separately dosed, calciothermic, aluminothermic, and slag analogues.

The most important design variable is not nominal wt.% Ca. Meaningful comparison requires total nominal oxygen-removal equivalents, calcium share of nominal reducing capacity, temperature, pressure, phase state, and closed Ca/Al/O balances. R_eq and χCa are normalization descriptors for comparison, not validated predictors of conversion, recovery, yield, or purity.

Intermediate phases are central to kinetics and product formation, but their roles are system-specific. Ca-bearing oxides, suboxides, aluminides, and intermetallics can open new reaction pathways, form diffusion barriers, or retain target metal; therefore, disappearance of the feed oxide cannot be equated automatically with recoverable metal.

Slag engineering is a principal reason to consider Ca–Al because coupled CaO and Al_2O_3 formation can move the oxide phase toward a more separable calcium-aluminate-rich melt. The benefit is conditional: liquidus relative to process temperature, solid fraction, viscosity, density contrast, wetting, droplet coalescence, and refractory dissolution must be evaluated together, without assuming a universal numerical process window.

The practical optimum is a multidimensional operating window balancing reduction strength, useful reaction heat, Ca retention, slag fluidity, metal coalescence, refractory compatibility, safety, and product purity. A higher Ca fraction is not inherently better. Ca–Al should be selected only when its coupled benefits in redox strength, heat balance, product purity, or slag separation outweigh volatility, containment, refractory, and safety burdens; otherwise pure Ca, conventional aluminothermy, or a modified slag route may be simpler and more defensible.

CC BY

JIRRS
Journal International Review of Research Studies

Received: 02/05/2026 - **Accepted:** 26/08/2026
Vol: 01.09
DOI: 10.66104/bn5j2634
Pages: 1-49

Industrial development should proceed from activity-informed thermodynamic screening to phase-resolved laboratory experiments and sealed pilot trials with closed Ca/off-gas balances and mandatory safety gates. The A–T–P–S–Q and scale-up frameworks are proposed decision aids that require prospective validation across chemically distinct systems. Environmental and economic superiority is not established here; future TEA/LCA should use an on-spec-metal functional unit and include reductant production, Ca losses, containment, refractory life, refining, off-gas treatment, recovery, and slag or coproduct credits.

Declarations

Funding: No external funding was received for this work.

Conflict of interest: The author declares no conflict of interest.

Author contributions: The sole author was responsible for conceptualization, critical synthesis, framework development, evidence classification, and writing.

Data availability: No new dataset was generated; all evidence is from the cited published literature.

References

Amon, A., Moore, E. E., Henderson, H. B., Shittu, J., Kunz, M., Kastamo, S., Huotari, N., Loukus, A., Ott, R., Weiss, D., & McCall, S. K. (2024). Aluminothermic reduction of CeO_2: Mechanism of an economical route to aluminum–cerium alloys. Materials Horizons, 11(10), 2382–2387. https://doi.org/10.1039/D4MH00087K

Athelli, A. R., & Reddy, R. G. (2026). Calciothermic reduction of samarium oxide to samarium. In The Minerals, Metals & Materials Society (Ed.), TMS 2026 155th Annual Meeting & Exhibition supplemental proceedings (pp. 1105–1113). Springer Nature Switzerland. https://doi.org/10.1007/978-3-032-13828-6_91

Azof, F. I., Tang, K., You, J., & Safarian, J. (2020). Synthesis and characterization of $12CaO{\cdot}7Al_2O_3$ slags: The effects of impurities and atmospheres on the phase relations. Metallurgical and Materials Transactions B, 51, 2689–2710. https://doi.org/10.1007/s11663-020-01969-8

Balakirev, V. F., Osinkina, T. V., Krasikov, S. A., Zhilina, E. M., Vedmid', L. B., & Zhidovinova, S. V. (2021). Joint metallothermic reduction of titanium and rare refractory metals of Group V. Russian Journal of Non-Ferrous Metals, 62(2), 190–196. https://doi.org/10.3103/S1067821221020024

Blenau, L. W., Vogt, D., Lonski, O., Abrar, A., Fabrichnaya, O., & Charitos, A. (2023). Development of a process to recycle NdFeB permanent magnets based on the CaO–

JIRRS
Journal International Review of Research Studies

Received: 02/05/2026 - **Accepted:** 26/08/2026
Vol: 01.09
DOI: 10.66104/bn5j2634
Pages: 1-49

Al_2O_3–Nd_2O_3 slag system. Processes, 11(6), Article 1783. https://doi.org/10.3390/pr11061783

Bullón, J., Crego, Ó., Ferrín, J. L., Gómez, D., Martínez, I., & Pérez-Pérez, L. J. (2025). Separation time of aluminothermic reduction products for sustainable silicon production. Open Research Europe, 4, Article 249. https://doi.org/10.12688/openreseurope.18833.2

Cai, T., Zhang, Y., Zheng, S., & Zhang, Y. (2026). Reaction pathway of the CaO- and $CaCl_2$-assisted aluminothermic reduction of TiO_2 for the precise fabrication of Ti_2O. Metallurgical and Materials Transactions B, 57(3), 1538–1549. https://doi.org/10.1007/s11663-025-03937-6

Cheng, C., Song, K.-X., Song, Z.-W., Wang, L.-F., Xu, Q.-Q., Zhang, L.-L., Han, C., Dou, Z.-H., & Zhang, T.-A. (2022). Synthesis of as-cast WCu composite containing micro- and nano-size tungsten particles using aluminothermic reduction. JOM, 74(3), 931–937. https://doi.org/10.1007/s11837-021-05047-5

Cheng, C., Song, Z.-W., Song, K.-X., Wang, L.-F., Huang, T., Zhou, Y.-J., Liu, H.-T., Li, S.-L., Han, C., Dou, Z.-H., & Zhang, T.-A. (2022). In-situ synthesis and characterizations of a novel aluminum bronze composite reinforced with micro-size tungsten particles. JOM, 74(11), 4146–4153. https://doi.org/10.1007/s11837-022-05311-2

Cheng, C., Song, Z.-W., Wang, L.-F., Song, K.-X., Huang, T., Zhao, L., Wang, L.-S., Dou, Z.-H., & Zhang, T.-A. (2022). Novel synthesis of CuW composite reinforced with lamellar precipitates via aluminothermic reduction. Rare Metals, 41(12), 4047–4054. https://doi.org/10.1007/s12598-022-02092-0

Cheng, C., Wang, X., Song, K., Song, Z., Dou, Z., Zhang, M., Liu, H., Li, X., & Niu, L. (2023). Effects of CaO addition on the CuW composite containing micro- and nano-sized tungsten particles synthesized via aluminothermic coupling with silicothermic reduction. Nanotechnology Reviews, 12(1), Article 20220527. https://doi.org/10.1515/ntrev-2022-0527

Cheng, C., Wang, X.-Y., Zhang, T.-A., Dou, Z.-H., Song, K.-X., Wang, M.-X., Feng, Y.-S., Huang, T., Liu, H.-T., Li, X.-H., & Li, K. (2024). Metal-slag separation strengthening through in situ slagging during CuW composite preparation by metallothermic reduction. Rare Metals, 43(11), 6113–6121. https://doi.org/10.1007/s12598-024-02820-8

Coetsee, T., & De Bruin, F. (2026). Sodium-oxide fluxed slag design, phase chemistry and thermochemistry calculations for aluminium recycling from aluminothermic reduction of manganese ore. Crystals, 16(6), Article 401. https://doi.org/10.3390/cryst16060401

CC BY

JIRRS
Journal International Review of Research Studies

Received: 02/05/2026 - **Accepted:** 26/08/2026
Vol: 01.09
DOI: 10.66104/bn5j2634
Pages: 1-49

Coetsee, T., De Bruin, F., Komarov, O., Popov, A., & Khudyakova, V. (2026). Thermochemical simulation of scheelite–millscale aluminothermy reactions in tungsten-alloyed steel production. Reactions, 7(2), Article 36. https://doi.org/10.3390/reactions7020036

de Oliveira, J. M., Anes, I. A., Coleti, J. L., Espinosa, D. C. R., de Carvalho, M. S., & Tenório, J. A. S. (2023). Niobium and tantalum recovery from the primary source and from tin slag, an industrial challenge: A review. The Canadian Journal of Chemical Engineering, 101(4), 1743–1761. https://doi.org/10.1002/cjce.24621

Deng, X.-L., Cheng, Y.-W., He, F.-L., Lv, Z.-P., Li, S.-L., He, J.-L., & Song, J.-X. (2026). Role of precursor and in situ mechanistic elucidation in metallothermic reduction reaction. Tungsten, 8(2), 289–313. https://doi.org/10.1007/s42864-026-00372-1

Disconzi, F., Bellotto, M., Frazzetto, R., Brunelli, K., Ardit, M., & Artioli, G. (2025). Aluminothermic recovery of strategic ferroalloys from ladle slag: An integrated thermodynamic and experimental approach. Minerals, 15(11), Article 1121. https://doi.org/10.3390/min15111121

Ellingham, H. J. T. (1944). Reducibility of oxides and sulphides in metallurgical processes. Journal of the Society of Chemical Industry, 63, 125–133.

Emil-Kaya, E., Sørli, F., Wallin, M., & Tranell, G. (2024, June 17–19). Refining of Si-Ca-Al alloys using slag treatments [Conference presentation]. 12th International Conference on Molten Slags, Fluxes and Salts (MOLTEN 2024), Brisbane, Australia.

Fu, D.-X., Wang, Y.-W., Di, Y.-Z., Peng, J.-P., & Feng, N.-X. (2024). Factors affecting reduction efficiency in industrial retorts for Mg production by aluminothermic process. Transactions of Nonferrous Metals Society of China, 34(4), 1288–1299. https://doi.org/10.1016/S1003-6326(24)66471-X

Geng, R., Li, J., & Shi, C. (2020). Evolution of calcium aluminate inclusions by cerium treatment in Al-killed steel during Ruhrstahl–Heraeus refining process. Steel Research International, 91(9), Article 2000117. https://doi.org/10.1002/srin.202000117

Gorkunov, V., & Munter, R. (2007). Calcium–aluminothermal production of niobium and mineral composition of the slag. Proceedings of the Estonian Academy of Sciences: Chemistry, 56(3), 142–156. https://doi.org/10.3176/chem.2007.3.04

Gulyaeva, R. I., Sergeeva, S. V., Petrova, S. A., & Udoeva, L. Yu. (2022). Calciothermic reduction of iron and manganese tantalates. Inorganic Materials: Applied Research, 13(2), 536–542. https://doi.org/10.1134/S2075113322020162

CC BY

JIRRS
Journal International Review of Research Studies

Received: 02/05/2026 - **Accepted:** 26/08/2026
Vol: 01.09
DOI: 10.66104/bn5j2634
Pages: 1-49

Gulyaeva, R. I., Udoeva, L. Yu., Petrova, S. A., Sergeeva, S. V., Pikulin, K. V., & Agafonov, S. N. (2022). Phase transformation during metallothermic reduction of tantalite. Metallurgist, 66(1–2), 200–214. https://doi.org/10.1007/s11015-022-01316-z

Guo, X.-Y., Dong, Z.-W., Xia, Y., Liu, P.-D., Liu, H.-N., & Tian, Q.-H. (2022). Preparation of low-oxygen-containing Ti–48Al–2Cr–2Nb alloy powder by direct reduction of oxides. Transactions of Nonferrous Metals Society of China, 32(4), 1351–1361. https://doi.org/10.1016/S1003-6326(22)65858-8

Guryanov, A. M., Yudin, S. N., Kasimtsev, A. V., Volodko, S. S., Alimov, I. A., & Evstratov, E. V. (2023). Kinetics and mechanism of calcium hydride synthesis of the intermetallic compound Cr_2Ta. Inorganic Materials, 59(5), 463–474. https://doi.org/10.1134/S0020168523050059

Huang, J., Zhang, L., Yu, W., Chen, J., Li, X., Li, Q., Liao, T., & Mo, X. (2025). Recovery of rare earth elements from calciothermic reduction slag by sulfation roasting–water leaching method. Minerals, 15(10), Article 1025. https://doi.org/10.3390/min15101025

Huo, G., Qiu, J., & Liu, C. (2026). Experimental study on phase equilibria of $CaO–Al_2O_3–La_2O_3$ system at 1873 and 1773 K. Journal of the American Ceramic Society, 109(2), Article e70534. https://doi.org/10.1111/jace.70534

Islam, M. K., Pownceby, M. I., Somerville, M., Tardio, J., Haque, N., & Bhargava, S. K. (2022). Effect of B_2O_3 on the liquidus temperature and phase equilibria in the $CaO–Al_2O_3–SiO_2–B_2O_3$ slag system, relevant to the smelting of e-waste. Journal of Sustainable Metallurgy, 8(4), 1590–1605. https://doi.org/10.1007/s40831-022-00581-1

Islam, M. K., Somerville, M., Pownceby, M. I., Tardio, J., Bhargava, S., & Haque, N. (2024). Experimental phase equilibria and liquidus of $CaO–Al_2O_3–SiO_2–Na_2O–B_2O_3$ slags relevant to e-waste processing. Metallurgical and Materials Transactions B, 55(1), 216–228. https://doi.org/10.1007/s11663-023-02952-9

Jain, U., & Awasthi, A. (2025). The use of Al_2O_3 as heat-sink during vanadium extraction by thermite process. Mineral Processing and Extractive Metallurgy, 134(1), 33–42. https://doi.org/10.1177/25726641241312789

Jiang, D., Zhao, Z., Tang, H., Zhang, H., Wang, R., Che, Y., & He, J. (2026). Research status and progress on preparation and purification of niobium metal by pyrometallurgy. Rare Metal Materials and Engineering, 55(8), 1917–1928. https://doi.org/10.12442/j.issn.1002-185X.20250397

CC BY

JIRRS
Journal International Review of Research Studies

Received: 02/05/2026 - **Accepted:** 26/08/2026
Vol: 01.09
DOI: 10.66104/bn5j2634
Pages: 1-49

Karati, A., Parmar, H., Riedemann, T., Besser, M., Prodius, D., & Nlebedim, I. C. (2025). Rare earth metals production using alternative feedstock that eliminates HF. Nature Communications, 16, Article 4528. https://doi.org/10.1038/s41467-025-59468-w

Kasimtsev, A. V., Levinsky, Yu. V., & Yudin, S. N. (2020). Calciothermic powders of rare metals and intermetallic compounds. Non-Ferrous Metals, (2), 31–50. https://doi.org/10.17580/nfm.2020.02.05

Khomenko, N. Yu., Konovalikhin, S. V., Chuev, I. I., Guda, S. A., Silyakov, S. L., & Kovalev, D. Yu. (2020). X-ray diffraction study of a new phase in the Ni–W–C system. Inorganic Materials, 56(6), 572–576. https://doi.org/10.1134/S0020168520060072

Kim, T. S., & Park, J. H. (2020). Thermodynamics of iron redox equilibria and viscosity-structure relationship of $CaO–Al_2O_3–Fe_tO$ melts. Journal of Non-Crystalline Solids, 542, Article 120089. https://doi.org/10.1016/j.jnoncrysol.2020.120089

Kim, T., & Lim, J.-W. (2022). Surface characterization of Ti and Ti–6Al–4V alloy by Ca vapor deoxidation: Relation between surface morphology and deoxidation reaction. Applied Surface Science, 590, Article 153098. https://doi.org/10.1016/j.apsusc.2022.153098

Kotschote, N. L., Bauer, N. M., Klar, P. J., & Ebbinghaus, S. G. (2026). Effects of niobium substitution on crystal structure and physical properties of mayenite $Ca_{12}Al_{14}O_{33}$. Journal of Physics and Chemistry of Solids, 213, Article 113602. https://doi.org/10.1016/j.jpcs.2026.113602

Kroll, W. (1937). Verformbares Titan und Zirkon. Zeitschrift für Anorganische und Allgemeine Chemie, 234(1), 42–50. https://doi.org/10.1002/zaac.19372340105

Kryzhanov, M. V., & Orlov, V. M. (2023). Calcium vapor reduction of niobium oxide compounds. Inorganic Materials, 59(11), 1250–1260. https://doi.org/10.1134/S0020168523110079

Kudyba, A., Akhtar, S., Johansen, I., & Safarian, J. (2021). Aluminothermic reduction of manganese oxide from selected MnO-containing slags. Materials, 14(2), Article 356. https://doi.org/10.3390/ma14020356

Kulu, P., Goljandin, D., Traksmaa, R., Kaljuvee, T., & Gregor, A. (2021). Thermal properties of calcium-aluminate based materials. IOP Conference Series: Materials Science and Engineering, 1140(1), Article 012028. https://doi.org/10.1088/1757-899X/1140/1/012028

Lee, B. P., Choi, J. S., Ko, J. W., Park, J. G., Min, D. J., & Sohn, I. (2024). Metallothermic reduction of Sc_2O_3 using Al–Ca alloys equilibrated with $CaO–CaCl_2$ flux. Journal of

CC BY

JIRRS
Journal International Review of Research Studies

Received: 02/05/2026 - **Accepted:** 26/08/2026
Vol: 01.09
DOI: 10.66104/bn5j2634
Pages: 1-49

Materials Research and Technology, 28, 327–334. https://doi.org/10.1016/j.jmrt.2023.11.283

Li, J., Hao, Z., Shu, Y., & He, J. (2020). Fabrication of spherical Ti–6Al–4V powder for additive manufacturing by radio frequency plasma spheroidization and deoxidation using calcium. Journal of Materials Research and Technology, 9(6), 14792–14798. https://doi.org/10.1016/j.jmrt.2020.10.054

Liu, C., Xie, X., Qiu, J., Li, W., & Huo, G. (2024a). Phase diagram of $CaO–Al_2O_3–VO_x$ slag system under reducing atmosphere. JOM, 76(11), 6555–6567. https://doi.org/10.1007/s11837-024-06866-y

Liu, C., Xie, X., Qiu, J., Li, W., & Huo, G. (2024b). The phase diagram of a $CaO–Al_2O_3–VO_x$ slag system under argon atmosphere at 1500 °C. Metals, 14(1), Article 108. https://doi.org/10.3390/met14010108

Ma, W., Wang, C., Xu, J., & Yin, R. (2025). Influence of the MgO content and the CaO/Al_2O_3 ratio on the structure and transport properties of molten $CaO–Al_2O_3–MgO$ slag systems: A molecular dynamics study. Metallurgical and Materials Transactions B, 56(5), 5821–5834. https://doi.org/10.1007/s11663-025-03736-z

Makhambetov, Y., Akhmetov, A., Smagulov, A., Sadyk, Z., Kabylkanov, S., Saulebek, Z., & Toleukadyr, R. (2026). Smelting of a complex W-, Mo-, and Cr-containing alloy in an induction furnace via metallothermic reduction. Alloys, 5(2), Article 11. https://doi.org/10.3390/alloys5020011

Makrovets, L. A., Samoilova, O. V., Bakin, I. V., & Mikhailov, G. G. (2022). Thermodynamic analysis of the deoxidation ability of alkaline-earth metals in the presence of aluminum. Russian Metallurgy (Metally), 2022(6), 575–582. https://doi.org/10.1134/S0036029522060180

Ming, G., Li, S., Zhang, Y., Lei, Y., Ren, Y., Lv, G., Wei, K., & Ma, W. (2025). A new method for producing Al–Si–Ca alloys, AlF_3, and MgF_2 using diamond wire saw Si powder and $CaF_2–MgO$ waste slag. Silicon, 17(7), 1555–1569. https://doi.org/10.1007/s12633-025-03287-7

Moura, V. V., Santos, T., & Pereira, C. (2022). Study of aluminothermic slag leaching for uranium and thorium recovery. Brazilian Journal of Radiation Sciences, 10(3B), 1–13. https://doi.org/10.15392/2319-0612.2022.2002

Nababan, D. C., Nuraeni, B. A., Rhamdani, A. R., Pownceby, M. I., & Rhamdhani, M. A. (2026). Metallothermic reduction using aluminum for metal and alloy production. International Materials Reviews. Advance online publication. https://doi.org/10.1177/09506608261467561

CC BY

JIRRS
Journal International Review of Research Studies

Received: 02/05/2026 - **Accepted:** 26/08/2026
Vol: 01.09
DOI: 10.66104/bn5j2634
Pages: 1-49

National Fire Protection Association. (2022). NFPA 484: Standard for combustible metals. National Fire Protection Association.

Okabe, T. H. (2020). Metallothermic reduction of TiO_2. In Z. Z. Fang, F. H. Froes, & Y. Zhang (Eds.), Extractive metallurgy of titanium: Conventional and recent advances in extraction and production of titanium metal (pp. 131–164). Elsevier. https://doi.org/10.1016/B978-0-12-817200-1.00008-9

Orlov, V. M., & Kryzhanov, M. V. (2020). Calcium reduction of zirconium oxide compounds. Inorganic Materials, 56(7), 734–738. https://doi.org/10.1134/S0020168520070122

Orlov, V. M., & Kryzhanov, M. V. (2021). Calciothermic reduction of titanium oxide compounds. Inorganic Materials, 57(1), 30–37. https://doi.org/10.1134/S0020168520120134

Orlov, V. M., & Kryzhanov, M. V. (2024). Comparison of the pore structure of calciothermic and magnesiothermic niobium and tantalum powders. Inorganic Materials, 60(13), 1426–1437. https://doi.org/10.1134/S0020168525700165

Ortega, J. N., Rupp, B., & Han, F. D. (2026). A review and analysis of extraction methods for aluminum and oxygen from lunar regolith. Space and Planetary Resources, 2, Article 5. https://doi.org/10.1007/s44461-026-00010-1

Palumbo, A. W., & Chubukov, B. A. (2023). Reductant considerations in thermal pathways to primary magnesium metal production: A case for aluminothermic reduction. In S. Barela, A. Leonard, P. Maier, N. R. Neelameggham, & V. M. Miller (Eds.), Magnesium technology 2023 (pp. 7–9). Springer. https://doi.org/10.1007/978-3-031-22645-8_2

Pastor-Vallés, E., Abadías Llamas, A., & Pettersen, J. B. (2025). Carbon-neutral silicon via aluminothermic reduction? Exploring industrial symbiosis through life cycle assessment. ACS Sustainable Chemistry & Engineering, 13(36), 14893–14902. https://doi.org/10.1021/acssuschemeng.5c04666

Pereira, A. C. (2026). Liquid-metal droplet coalescence in metallurgical slags: A critical review of interfacial phenomena, slag properties, hydrodynamics, kinetics, and metal recovery. International Journal of Research and Scientific Innovation, 10(7), 15007–15036. https://doi.org/10.47772/IJRISS.2026.100701023

Philipson, H. G. R., Wallin, M., & Einarsrud, K. E. (2024a). Aluminothermic reduction kinetics of calcium silicate slag for silicon alloy production. Metals, 14(6), Article 604. https://doi.org/10.3390/met14060604

Philipson, H. G. R., Wallin, M., & Einarsrud, K. E. (2024b). Investigation of liquid–liquid reaction phenomena of aluminum in calcium silicate slag. Materials, 17(7), Article 1466. https://doi.org/10.3390/ma17071466

CC BY

JIRRS
Journal International Review of Research Studies

Received: 02/05/2026 - **Accepted:** 26/08/2026
Vol: 01.09
DOI: 10.66104/bn5j2634
Pages: 1-49

Pikulin, K. V., Galkova, L. I., Gulyaeva, R. I., Udoeva, L. Yu., Sergeeva, S. V., & Tyushnyakov, S. N. (2026). Phase formation features during metallothermic reduction of natural wolframite. Non-Ferrous Metals, (1), 9–19. https://doi.org/10.17580/nfm.2026.01.02

Pikulin, K. V., Tyushnyakov, S. N., Gulyaeva, R. I., Petrova, S. A., Dmitriev, A. N., & Vitkina, G. Yu. (2026). Phase formation features in the metallothermal reduction of natural coltan. Metals, 16(4), Article 436. https://doi.org/10.3390/met16040436

Qiu, J., Jiang, J., Xie, X., Li, W., & Liu, C. (2023). Phase diagram of $CaO–Al_2O_3–V_2O_5$ slag system at 1500 °C and 1600 °C. Journal of Sustainable Metallurgy, 9(3), 1010–1019. https://doi.org/10.1007/s40831-023-00704-2

Rafique, M. M. A. (2024). Pyrometallurgy and electrometallurgy of rare earths–Part A: Analysis of metallothermic reduction and its variants. Mineral Processing and Extractive Metallurgy Review, 45(4), 389–396. https://doi.org/10.1080/08827508.2022.2164576

Rasheed, M. Z., Dahm, K., Hunter-Smith, G., Pistidda, C., & Bumby, C. (2026). Optimizing the yield of TiFe intermetallic compound from direct calciothermic reduction of ilmenite sand. Journal of Alloys and Compounds, 1058, Article 187019. https://doi.org/10.1016/j.jallcom.2026.187019

Ren, L., Le, Q., Gao, S., Wei, X., Yin, Z., Liao, Q., & Li, Y. (2025). Thermodynamics and kinetics of preparation of Y-containing magnesium alloy by calciothermic reduction in Mg–Ca melt. Metallurgical and Materials Transactions B, 56(3), 2332–2349. https://doi.org/10.1007/s11663-025-03488-w

Sahoo, D. K., Sarode, P. S., Ambare, D. N., Mondal, S., & Singh, D. K. (2024). Study on the extraction of neodymium metal by calciothermic reduction process. Mineral Processing and Extractive Metallurgy, 133(3), 101–108. https://doi.org/10.1177/25726641241276483

Sergeeva, S. V., Gulyaeva, R. I., Udoeva, L. Yu., Petrova, S. A., & Tyushnyakov, S. N. (2022). Thermodynamic simulation and experimental investigation of the calciothermic reduction of metals from manganese and iron niobates. Russian Metallurgy (Metally), 2022(8), 909–918. https://doi.org/10.1134/S0036029522080146

Sohn, H.-S. (2026). Smelting and recycling of tantalum. Resources Recycling, 35(1), 3–16. https://doi.org/10.7844/kirr.2026.35.1.3

Song, Y., Dou, Z., Zhang, T.-A., & Wang, G. (2021). Mechanisms of metal-slag separation behavior in thermite reduction for preparation of TiAl alloy. Journal of Materials Engineering and Performance, 30(12), 9315–9325. https://doi.org/10.1007/s11665-021-06074-8

CC BY

JIRRS
Journal International Review of Research Studies

Received: 02/05/2026 - **Accepted:** 26/08/2026
Vol: 01.09
DOI: 10.66104/bn5j2634
Pages: 1-49

Su, K., Ma, X., & Zhao, B. (2021). Harmless treatment and valuable metals recovery of tungsten leaching residues: A thermodynamic and experimental study. JOM, 73(6), 1937–1946. https://doi.org/10.1007/s11837-021-04682-2

Su, Y., Duan, S., Kim, J., Kim, J.-K., & Park, J. H. (2026). Sustainable manufacturing of clean Ti-Ni alloy by remelting titanium scrap with calcium and halide fluxes. Metals and Materials International, 32(2), 734–748. https://doi.org/10.1007/s12540-025-01956-1

Suzuki, R. O., & Ono, K. (2025). Overview: OS process–I. Fundamental. Materials Transactions, 66(8), 913–925. https://doi.org/10.2320/matertrans.MT-M2024125

Teslia, M., Teslia, S., & Solodkyi, I. (2026). Synthesis of Mo–Ti–Ta–Cr alloy powders by calciothermic reduction. Journal of Manufacturing and Materials Processing, 10(7), Article 251. https://doi.org/10.3390/jmmp10070251

Turkdogan, E. T. (1983). Physicochemical properties of molten slags and glasses. The Metals Society.

Tyushnyakov, S. N., Gulyaeva, R. I., Udoeva, L. Yu., Sergeeva, S. V., & Petrova, S. A. (2021). Metallothermic reduction of natural cassiterite. Metallurgist, 65(7–8), 746–759. https://doi.org/10.1007/s11015-021-01212-y

Usta, M. C., Yörük, C. R., Uibu, M., Traksmaa, R., Hain, T., Gregor, A., & Trikkel, A. (2023). Carbonation and leaching behaviors of cement-free monoliths based on high-sulfur fly ashes with the incorporation of amorphous calcium aluminate. ACS Omega, 8(32), 29543–29557. https://doi.org/10.1021/acsomega.3c03286

Verein Deutscher Eisenhüttenleute. (1995). Slag atlas (2nd ed.). Verlag Stahleisen.

Volodin, A. M., Kenzhin, R. M., Kapishnikov, A. V., Komarovskikh, A. Yu., & Vedyagin, A. A. (2022). Aluminothermic synthesis of dispersed electrides based on mayenite: XRD and EPR study. Materials, 15(24), Article 8988. https://doi.org/10.3390/ma15248988

Wang, C., Xie, C., Xu, J., & Wan, K. (2025). Wettability and spreading kinetics between some refractory materials and molten calcium aluminate slag. Steel Research International, 96(9), 156–175. https://doi.org/10.1002/srin.202400895

Wang, F., Xu, B., Wan, H., Yang, J., Yang, B., & Jiang, W. (2020). Preparation of vanadium powders by calcium vapor reduction of V_2O_3 under vacuum. Vacuum, 173, Article 109133. https://doi.org/10.1016/j.vacuum.2019.109133

Wang, G., Nabeel, M., Dogan, N., Mu, W., & Phillion, A. B. (2025). Dissolution kinetics and mechanisms of calcium aluminate inclusions in $CaO–Al_2O_3–SiO_2–(MgO)$ steelmaking slags. Ceramics International, 51(24), 42315–42326. https://doi.org/10.1016/j.ceramint.2025.06.445

CC BY

JIRRS
Journal International Review of Research Studies

Received: 02/05/2026 - **Accepted:** 26/08/2026
Vol: 01.09
DOI: 10.66104/bn5j2634
Pages: 1-49

Wang, L. L., Munir, Z. A., & Maximov, Y. M. (1993). Thermite reactions: Their utilization in the synthesis and processing of materials. Journal of Materials Science, 28(14), 3693–3708. https://doi.org/10.1007/BF00353167

Wang, Y., Tang, H., Wang, K., Xiang, Q., Jia, X., & Zhang, J. (2026). A total calcium to total oxygen mass ratio control model based on Ca–Al–O ternary phase diagram and its application to calcium treatment process of Al-deoxidized steels. Metallurgical and Materials Transactions B. Advance online publication. https://doi.org/10.1007/s11663-026-04227-5

Xie, X., Liu, C., Qiu, J., Li, W., & Huo, G. (2025). Phase equilibrium of $CaO–Al_2O_3–VO_x$ system in air atmosphere at 1400 °C. Metallurgical and Materials Transactions B, 56(3), 2982–2992. https://doi.org/10.1007/s11663-025-03537-4

Xie, X., Liu, C., Qiu, J., Li, W., & Huo, G. (2026). Phase equilibrium study of $CaO–Al_2O_3–VO_x$ slag system under argon atmosphere at 1600 °C. Metallurgical and Materials Transactions B, 57(1), 680–692. https://doi.org/10.1007/s11663-025-03878-0

Yao, H., Zhuang, C., Li, C., Xiang, S., Li, X., Yang, G., & Zhang, Z. (2023). Study on the effect of calcium alloy on arsenic removal from scrap-based steel production. Materials, 16(8), Article 3113. https://doi.org/10.3390/ma16083113

Yuan, F., Zhao, Z., Zhang, Y., & Wu, T. (2022). Effect of Al_2O_3 content on the viscosity and structure of $CaO–SiO_2–Cr_2O_3–Al_2O_3$ slags. International Journal of Minerals, Metallurgy, and Materials, 29(8), 1522–1531. https://doi.org/10.1007/s12613-021-2306-2

Yudin, S. N., Volodko, S. S., Guryanov, A. M., Kasimtsev, A. V., Sviridova, T. A., Alimov, I. A., Kuzovchikov, S. N., Kondratiev, A. A., Korotitskiy, A. V., & Moskovskikh, D. O. (2024). Fabrication of refractory intermetallic Cr_2Ta by reducing metal oxides with calcium hydride. Metallurgical and Materials Transactions B, 55(3), 1261–1276. https://doi.org/10.1007/s11663-024-03018-0

Yudin, S. N., Volodko, S. S., Rumyantsev, B. A., Kotyakova, K. Yu., Moskovskikh, D. O., Markova, G. V., Evstratov, E. V., Guryanov, A. M., & Kasimtsev, A. V. (2026). Occurrence forms of light impurity elements in Cr–Ta powders produced by calciothermic reduction. International Journal of Refractory Metals and Hard Materials, 134, Article 107472. https://doi.org/10.1016/j.ijrmhm.2025.107472

Yudin, S., Volodko, S., Berdonosova, E., Klyamkin, S., Yermekova, Z., & Moskovskikh, D. (2025). Effect of synthesis parameters on the phase composition, purity, and structure of $LaNi_5$ powder produced by the calciothermic process. Journal of Alloys and Compounds, 1010, Article 178170. https://doi.org/10.1016/j.jallcom.2024.178170

CC BY

JIRRS
Journal International Review of Research Studies

Received: 02/05/2026 - **Accepted:** 26/08/2026
Vol: 01.09
DOI: 10.66104/bn5j2634
Pages: 1-49

Zeng, Y., Zhang, Y., Xue, N., Liu, H., & Zhang, Z. (2026). A novel electro-aluminothermic route to V–Ni alloys: $Ca_3(VO_4)_2$ as the vanadium source. RSC Advances, 16(35), 35950–35960. https://doi.org/10.1039/D6RA03772K

Zhang, L., Chen, M., & Sun, X. (2022). Evolution of viscosity and structural properties during aluminothermic reduction of vanadium-enriched slag. Steel Research International, 93(6), Article 2100738. https://doi.org/10.1002/srin.202100738

Zhang, X., Liu, C., & Jiang, M. (2022). Effect of B_2O_3 addition and CaO/Al_2O_3 ratios on melt structure and viscosity of $CaO–Al_2O_3$-based slags. Metals, 12(8), Article 1255. https://doi.org/10.3390/met12081255

Zhi, W., Wang, F.-Y., Chen, X., Tian, Y., & Yang, B. (2022). Thermodynamic assessment of the $CaO–Al_2O_3–Sc_2O_3$ ternary system. Calphad, 78, Article 102454. https://doi.org/10.1016/j.calphad.2022.102454

Zhu, M., & Safarian, J. (2023). Alumina production from $CaO–Al_2O_3–SiO_2$ slag produced in SisAl process. In TRAVAUX 52: Proceedings of the 41st International ICSOBA Conference (pp. 499–509). ICSOBA.

Zhu, M., Philipson, H., Blandhol, K., Djupvik, V., Engvoll, K., Safarian, J., Tang, K., Görnerup, M., Pastor-Vallés, E., Wallin, M., & Tranell, G. (2024). Pilot-scale aluminothermic production of silicon alloy and alumina-rich slag. ACS Sustainable Chemistry & Engineering, 12(40), 14795–14809. https://doi.org/10.1021/acssuschemeng.4c05326

CC BY